AAPM SCIENTIFIC REPORT

MEDICAL PHYSICS

AAPM Task Group Report 272: Comprehensive acceptance testing and evaluation of fluoroscopy imaging systems

Pei-Jan Paul Lin[1] | Allen R. Goode[2] | Frank D. Corwin[1] | Ryan F. Fisher[3] | Stephen Balter[4] | Kevin A. Wunderle[5] | Beth A. Schueler[6] | Don-Soo Kim[7] | Jie Zhang[8] | Yifang (Jimmy) Zhou[9] | Peter A. Jenkins[10] | Usman Mahmood[11] | Teh Lin[12] | Hui Zhao[13] | Mi-Ae Park[14] | Annalisa Trianni[15] | Markus Lendle[16] | Andrew Kuhls-Gilcrist[17] | Jan C. Jans[18] | Lionel Desponds[19] | Gene Banasiak[20] | Steve Backes[21] | Carl Snyder[21] | Angela Snyder[21] | Minghui Lu[22] | Scott Gonzalez[23]

[1] Department of Radiology, Virginia Commonwealth University, Richmond, Virginia, USA

[2] Department of Radiology, University of Virginia, Charlottesville, Virginia, USA

[3] Department of Radiology, The MetroHealth System, Cleveland, Ohio, USA

[4] Departments of Medicine and Radiology, Columbia University Medical Center, New York, New York, USA

[5] Department of Radiology, Cleveland Clinic, Cleveland, Ohio, USA

[6] Radiology Department, Mayo Clinic, Rochester, Minnesota, USA

[7] Department of Radiology, Boston Children's Hospital and Harvard Medical School, Boston, Massachusetts, USA

[8] Department of Radiology, University of Kentucky, Lexington, Kentucky, USA

[9] Department of Imaging, Cedars-Sinai Medical Center, Los Angeles, California, USA

[10] Department of Radiology, University of Utah Health, Salt Lake City, Utah, USA

[11] Department of Medical Physics, Memorial Sloan Kettering Cancer Center, New York, New York, USA

[12] Department of Radiation Oncology, Fox Chase Cancer Center, Philadelphia, Pennsylvania, USA

[13] Department of Radiation Oncology, University of Utah, Salt Lake City, Utah, USA

[14] Department of Radiology, University of Texas Southwestern, Dallas, Texas, USA

[15] Medical Physics Department, Udine University Hospital, Udine, Italy

[16] Siemens Healthcare, Forchheim, Germany

[17] Canon Medical Systems USA, Inc., Tustin, California, USA

[18] Philips Healthcare, Best, The Netherlands

Acronyms: AAPM, American Association of Physicists in Medicine; ACR, American College of Radiology; ADRC, Automatic dose rate control; AKR, Air kerma rate; AP, Anteroposterior (anterior–posterior); AR, Ambience ratio (L_{amb}/L_{min}); CA, Caudal; CNR, Contrast-to-noise ratio; CR, Cranial; CT, Computed tomography; CVIA, Cardiovascular-visceral interventional angiography; DAP, Dose-area product (see KAP); DICOM®, Digital imaging and communications in medicine; FGI, Fluoroscopically-guided intervention; FOV, Field of view; FPIR, Flat panel image receptor; GI, Gastrointestinal; HT, High tension; HVAC, Heating, ventilation air conditioning; HVL, Half-value layer (mm Al); IDRIR, Input dose rate to the image receptor; IEC, International Electrotechnical Commission; II, Image intensified, image intensifier; IPEM, Institute of Physics and Engineering in Medicine; IR, Image receptor; IR, Interventional radiology; IRID, Image receptor input dose; IRP, Interventional reference point (see PERP); IXE, Interventional X-ray equipment; $K_{air,PERP}$, Air kerma at PERP; KAP, Air-kerma-area product (also see DAP); kV_{anode}, Tube potential measured at anode versus ground; kV_{cathod}, Tube potential measured at cathode versus ground; KVD, kV detector; KVS, kV source; kV_{total}, Tube potential measured across anode and cathode; L'_{max}, Total maximum combined luminance; $L_{max} + L_{amb}$; L'_{min}, Total minimum combined luminance; $L_{min} + L_{amb}$; L_{amb}, Ambient luminance; LAO, Left anterior oblique; LINAC, Linear accelerator; L_{max}, Maximum luminance; L_{min}, Minimum luminance; LR, Luminance ratio; L'_{max}/L'_{min}; LUDM, Luminance uniformity deviation from the median; MPPG, Medical physics practice guideline; NEMA, National Electrical Manufacturers Association; Non-II, NonImage Intensified; PA, Postero-anterior (posterioranterior); PACS, Picture archiving and communications system; PERP, Patient entrance reference point; PMMA, Polymethyl methacrylate; PPS, Pulse per second; PSD, Patient skin dose; QC, Quality control; QMP, Qualified medical physicist; RAO, Right anterior oblique; R_d, Diffuse reflection coefficient; RDIM, Radiation dose index monitoring; RDSR, Radiation Dose Structured Report; RFIRC, Radiation field to image receptor congruence; RP, Reference point (see PERP); SDD, Source-to-Detector Distance; SDNR, Signal difference to noise ratio; SID, Source-to-image receptor distance; SIIM, Society for Imaging Informatics in Medicine; SMPTE, Society of Motion Picture and Television Engineers; SNR, Signal-to-noise ratio; SSD, Source-to-skin distance; SSDS, Solid-state detector system; SSF, Spectral shaping filter; TJC, The Joint Commission

[19] General Electric Healthcare, Buc, France

[20] Clinical Micro Systems, Arlington, Virginia, USA

[21] Atirix Medical Systems, Inc., Minneapolis, Minnesota, USA

[22] Varex Imaging Corporation, San Jose, California, USA

[23] Food and Drug Administration, Health and Human Services, Silver Spring, Maryland, USA

Correspondence
Pei-Jan Paul Lin, Department of Radiology,
Virginia Commonwealth University, Richmond,
VA 23298, USA.
Email: pei-jan.lin@vcuhealth.org

[Correction added on 4 Feb, 2022 after first
online publication: the title is updated.]

Abstract

Modern fluoroscopes used for image guidance have become quite complex. Adding to this complexity are the many regulatory and accreditation requirements that must be fulfilled during acceptance testing of a new unit. Further, some of these acceptance tests have pass/fail criteria, whereas others do not, making acceptance testing a subjective and time-consuming task. The AAPM Task Group 272 Report spells out the details of tests that are required and gives visibility to some of the tests that while not yet required are recommended as good practice. The organization of the report begins with the most complicated fluoroscopes used in interventional radiology or cardiology and continues with general fluoroscopy and mobile C-arms. Finally, the appendices of the report provide useful information, an example report form and topics that needed their own section due to the level of detail.

KEYWORDS
acceptance tests, fluoroscopy, interventional angiography

1 | INTRODUCTION

The American Association of Physicists in Medicine (AAPM) Task Group (TG) 272 was established in November 2015 with the goal of defining testing procedures for fluoroscopic imaging systems, including conventional, mobile C-arm, and interventional/angiography systems, thereby establishing a comprehensive acceptance test procedure for practicing medical physicists. This test procedure would incorporate:

- regulatory tests and measurements such as those described in the National Electrical Manufacturers Association (NEMA) standard XR 27–2013, "X-ray Equipment for Interventional Procedures User Quality Control Mode,[1]"
- Current applicable International Electrical Commission (IEC) standards (IEC 60601-2-54:2009+AMD1:2015+AMD2:2018 CSV, consolidated version),[2] and
- image quality assessment accounting for new technological advancements in fluoroscopy equipment design.

1.1 | Disclaimer and precautions

The tests described in this report are recommended for acceptance testing to be performed by a Qualified Medical Physicist (QMP), as defined by AAPM Policy and Procedure 1-j (PP 1-j) and with the appropriate qualifications, as described in AAPM Medical Physics Practice Guideline 10 (AAPM Medical Physics Practice Guideline 10.a.: Scope of practice for clinical medical physics published in the *Journal of Applied Clinical Medical Physics [JACMP]*, 2018). However, many of these tests are beyond what might be needed for routine testing, and therefore, should not be considered as recommended for routine evaluations. Furthermore, the contents and tolerances described in this report should not be used as the basis for establishing regulatory or standards requirements for quality control (QC) testing.

In the United States, each state has regulatory authority over X-ray imaging system performance. As such, there is a wide range of regulatory requirements that may or may not be covered within this document. All

physicists performing regulatory testing of fluoroscopes must be sure to follow the requirements of the appropriate regulatory authority.

Digital image receptors are highly sensitive to sharp edges of radiation intensity in the radiation field. For many test devices, including radiation detectors, phantoms, and instruments, *it is strongly recommended that protective attenuators and/or proper collimation be provided for prolonged and/or repetitive exposures.* If such protection is not provided, permanent damage to the image receptor can occur. To this end, testers should not allow a bare unattenuated beam to occur adjacent to highly attenuating objects such as lead sheets or lead-lined detectors. At a minimum, depending on the X-ray energy under investigation, 3–5 mm of copper (Cu) sheets or 5–10 cm of polymethyl methacrylate (PMMA) plates should be used if the lead or other highly attenuating material does not adequately cover the entire surface of the image receptor.

1.2 | Acceptance testing versus commissioning of fluoroscopy systems

In the diagnostic radiology environment, imaging systems are often preconfigured and programmed at the factory for the intended application of the system. Application specialists from the vendors then visit the installation sites and fine-tune the examination protocols based on the preferences of the site's physicians. This fine-tuning process, in which imaging parameters are adjusted iteratively as users become more familiar with the new equipment, is part of the commissioning of a fluoroscopy system. TG 272 was not tasked with addressing the commissioning process, as it requires intimate knowledge of the medical procedures involved and in-depth experience regarding specific models of imaging equipment.

It is highly recommended that acceptance testing be performed before the imaging equipment is released for clinical use in patients.

Acceptance testing refers to the evaluation of a new piece of imaging equipment, and it is highly recommended that the evaluation occurs prior to clinical use. Typically, this process consists of tests designed to ensure the imaging equipment performs as expected, according to manufacturers' specifications and regulatory requirements. This includes evaluation of geometric accuracy of components (Section 2.2), radiation output (Section 2.3), image quality (Section 2.7), monitor performance (Section 2.5), and basic safety features and includes both quantitative measurements and qualitative analyses. Furthermore, periodic equipment testing should take place at regular intervals specified by the state after the equipment has been introduced into clinical use. Periodic testing generally consists of a subset of tests included in acceptance testing.

1.3 | Fluoroscopy systems included in this report

Previous Task Group efforts on fluoroscopy system evaluations and imaging equipment testing have focused on cardiovascular and visceral interventional angiography systems, or interventional X-ray equipment (IXE) according to IEC terminology, because of the mechanical sophistication of these systems and the complexity of their operation logic and electronic design. This report addresses IXE as the starting point in Section 2; however, the contents are expanded in the following sections to address all other fluoroscopy imaging systems, including:

- conventional fluoroscopes such as those employed in upper/lower gastrointestinal studies, with the X-ray tube assembly installed beneath the examination table;
- over-table X-ray tube fluoroscopes that may be operated remotely and may be used not only for upper/lower gastrointestinal studies but also for applications such as cystoscopy, endoscopy, and bronchoscopy;
- standard mobile C-arm (or full-size C-arm and Intra-operative 2D/3D) fluoroscopes employed in various disciplines of medicine;
- mobile mini C-arm systems typically used for imaging of extremities; and
- on-board imaging systems (OBIs) of therapeutic accelerators.

To avoid repetitive explanations, descriptions of items involved in testing IXE systems are provided in Section 2; thereafter, these items are not described again for other systems. In addition, items unique to a specific fluoroscopy system type are described in their respective sections. Additionally, boxes headed with **"NOTE"** appear throughout the text to provide further descriptions, delineate exceptions, or offer supplemental explanations.

This report is written to provide practical guidance regarding acceptance testing and periodic required regulatory evaluation of fluoroscopy systems. A suggested acceptance testing report is therefore presented as a guiding document, and the physical parameters to be tested and measurements required are discussed in detail when deemed necessary. However, a minimal amount of instruction is provided regarding, for instance, how to use the radiation probe-electrometer system to measure tube voltage and half-value layer (HVL). Additional information is provided in user manuals and basic radiation physics textbooks. In addition, AAPM TG 238 has been tasked with addressing the rotational angiography aspect of fluoroscopic operation; thus, this specific operational capability is not discussed in this report.

1.4 | Sample form

An example data collection form is attached as Appendix A. The sample form is only an example, and may be used as a starting point for data collection. The form is generic and not comprehensive for any particular fluoro system. Fluoroscopy systems differ substantially from one model to the next and are equipped with various operating modes with extensive "tree" structures based on the intended operation or examination type. Therefore, the sample form should by no means be considered a complete set of data to be acquired or used for analysis. The first two pages of the sample form also include a summary of test results and equipment-specific information such as serial numbers and available field size; when these data are readily available, system performance and specifications can be quickly assessed, and multiple similar units can be compared. Additionally, the specifics of geometrical setup and selected system parameters used for testing are recorded on the sample form. These factors are important to document, as changes in setup can lead to differences in longitudinal test results, even with no changes to the underlying system performance.

2 | INTERVENTIONAL X-RAY EQUIPMENT

2.1 | Mechanical factors

At the time of equipment installation, the examination table/pedestal assembly is mechanically aligned with the C-arm gantry. The alignment of the C-arm gantry and the examination table affects all other device settings such as lateral plane alignment, as well as positioning of auxiliary equipment such as video monitors and power injectors.

NOTE 1: The mechanical alignment should be evaluated at the time of acceptance testing; further assessment of this alignment may not be required on an annual basis. The mechanical alignment should also be evaluated whenever the C-arm is involved in a collision that may have resulted in mechanical misalignment and whenever corrective maintenance is performed to mechanical components associated with the C-arm and the examination table/pedestal. Therefore, the testing result may simply be "satisfactory" or "misalignment correction required." Readers should create their own forms for the evaluation of mechanical alignment especially when a misalignment is found. The issue can be as simple as a minor adjustment, or may be more complex, requiring a reset of the entire equipment layout.

The system microenvironment should be evaluated for completeness and readiness for operation. The medical physicist may want to review the report prepared by the installation engineer describing the conditions of the microenvironment in which the IXE is located. The microenvironment includes the areas surrounding the unit that may affect optimal operation. Many IXE systems have generator cabinets installed in separate rooms; temperature and humidity values should be evaluated in both the system and where generator is installed. The heating, ventilation, and air conditioning system may need to be adjusted if temperatures are outside of the system operation range specification. Stray magnetic fields should also be identified if the imaging unit is near a magnetic resonance imaging system, vendor installation documents will typically provide maximum magnetic field tolerances.

For newly installed units, the assumption is made that the required state and local codes regarding shielding plans and specifications have already been satisfied; however, a post build radiation protection survey may be required to ensure adequate shielding. The vendor may also supply an iso-dose map to illustrate scatter/stray radiation from the unit. This information can also be checked to ensure proper assembly from a radiation safety standpoint. The vendor's installation manual should be consulted for further details.

Two additional pieces of information regarding mechanical factors should be highlighted. First, vibrations caused by external mechanical and electrical equipment installed in the environment must be considered. If image quality issues are found during acceptance testing, characteristics of the microenvironment should be considered, including vibrations or stray magnetic fields as IXE systems are often placed in areas near large heating, ventilation, and air conditioning systems; air handler units; elevators; pumping stations; and so on. These building support utilities may transfer unwanted vibrations to the IXE system through the floor (table- and floor-mounted systems) or through the ceiling (ceiling-suspended C-arm systems). Such vibrations can be detected by placing a vessel containing a small amount of water on the system and looking for waves in the water surface.

If vibrations are of great enough magnitude, they may interfere with or add noise to the imaging chain. Figure 1 provides an example of a line-pair phantom imaged using the digital subtraction angiography (DSA) function on an IXE system. Figure 1(a) shows a DSA image obtained in the absence of mechanical vibration, whereas Figure 1(b) shows a DSA image obtained in the presence of a small vibration caused by an external mechanical or electrical source. In the image with the vibration, the misregistration of the mask and subsequent subtracted image is imperfect, causing a mismatch in the subtraction.
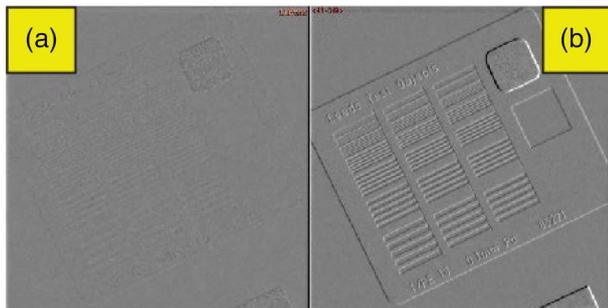
FIGURE 1 DSA images obtained in the absence of vibration (a) and in the presence of vibration (b). Note that the line pairs are more visible in the image on the right (b) because of errors in the registration of the subtraction process caused by the vibration

Because of this potential for image deterioration, any detected vibrations should be mitigated with dampeners or other shock-absorbing devices.

Second, a geometrical coordinate system as defined by Digital Imaging and Communications in Medicine (DICOM) should be considered (Figure 2).[3] According to DICOM convention, the long axis of the examination table (Z-axis) is defined as the lateral direction (Figure 2a), and the X-axis is defined as the longitudinal direction (Figure 2b); the white arrows in the figure indicate the positive direction. The Y-axis corresponds to the table-up (negative) and table-down (positive) motions. The origin $(X, Y, Z) = (0,0,0)$ is located at the isocenter of the C-arm gantry.

The signs of the primary and secondary rotations for the positioner (the C-arm gantry; often identified as the A-plane) are also shown in Figure 2. C-arm rotation about the X-axis is defined as secondary rotation; C-arm rotation about the Z-axis is defined as primary rotation. The direction of positive rotation is a left-handed turn for secondary rotation and a right-handed turn for primary rotation, and the 0° is in the negative Y direction, or at 12 o'clock. These geometrical parameters are recorded in the DICOM header for each acquired image, as well as in the Radiation Dose Structured Report (RSDR) for each acquired image and for each fluoroscopic pedal or button press (also known as an "event") during the procedure.

The geometric parameters recorded in the DICOM header are critically important when using either manufacturer-provided or third-party software to calculate peak patient skin dose (PSD). An understanding of the patient position on the table and precise table-gantry positions is needed to determine PSD. These table-gantry positional parameters include:

- the orientation of the patient on the examination table,
- the primary angulation of the X-ray source to the left or right of the patient,
- the secondary angulation of the X-ray source in the cranial or caudal plane of the patient,
- the X-ray source-to-image receptor distance (SID),
- the X-ray source-to-patient entrance distance,
- the longitudinal position of the patient relative to the X-ray source (patient left/right),
- the lateral position of the patient relative to the X-ray source (patient head/foot), and
- the manufacturer-specified patient entrance reference point (PERP) dose location between the source and image receptor.

The accuracy of the positional parameters listed above depends on proper alignment of the table with the center of rotation of the C-arm. Methods for verifying the accuracy of this alignment are provided in the following sections and in Appendix E.

2.1.1 │ Alignment of the examination table with the C-arm gantry

1. Ensure that all movable parts of the pedestal and tabletop (patient examination table) are at their default "park" location. In other words, all motions available should be set such that the tabletop (and pedestal if movable) is perpendicular to the primary axis of rotation and the angulation is set to 0°. Referring to Figure 3, at the head-end of the tabletop, measure the tabletop width "W," at two different locations (P_1 and P_2) about 20 cm apart. Determine and mark the centers as P_1 and P_2. Draw the centerline of the examination tabletop connecting P_1 and P_2 as shown in Figure 3(a) where W_H refers to the width measured at head end. A metal bar (approximately 5 mm in diameter and 40 cm in length) is affixed to the centerline with adhesive tape as shown in Figure 3(b). Similarly, repeat this process at the foot end of the table. Draw a line connecting P_3 and P_4 where W_F is the width measured at the foot end of the tabletop (Figure 3c).
2. Move the tabletop to a location typically employed for imaging the patient $(X, Y, Z) = (X, Y, Z_P)$.
3. Elevate the tabletop close to the gantry rotation central axis of $(X, Y, Z) = (X, 0, Z_P)$. With the positioner primary angle set to 0°, step on the fluoroscopy pedal. As the C-arm gantry rotating about the $Y = 0$ central axis, observe that the metal bar on the display monitor is located in the center of the image as shown in Figure 4.
4. Pan the tabletop in the XZ-plane such that the metal bar appears to be stationary in the center of the display monitor during C-arm rotation, refer to Figure 4. The metal bar should be located at $(X, Y, Z) = (0, 0, Z_P)$. Conversely, the table location indices should also show $(X, Y, Z) = (0, 0, Z_P)$. If this is not the case, the X- and Y-values must be recalibrated or readjusted by the service engineer. Lock the tabletop from moving
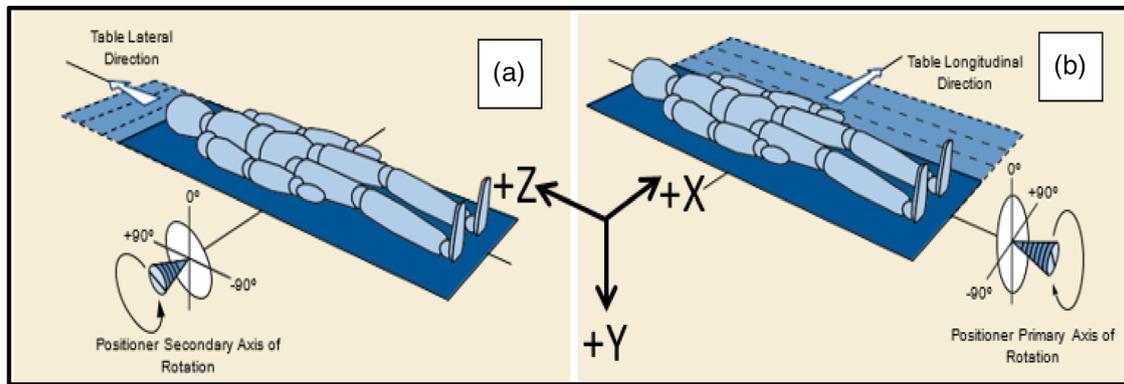
FIGURE 2 The definitions of DICOM geometrical coordinates for the lateral (a) and longitudinal (b) directions are depicted. The Cartesian coordinate system, including the positive direction of each axis, is also shown. Note that lowering the examination table is considered a move in the positive direction (+Y). (Adapted from DICOM PS 3.3 2014c Part 03, Section C8.7.4.1)
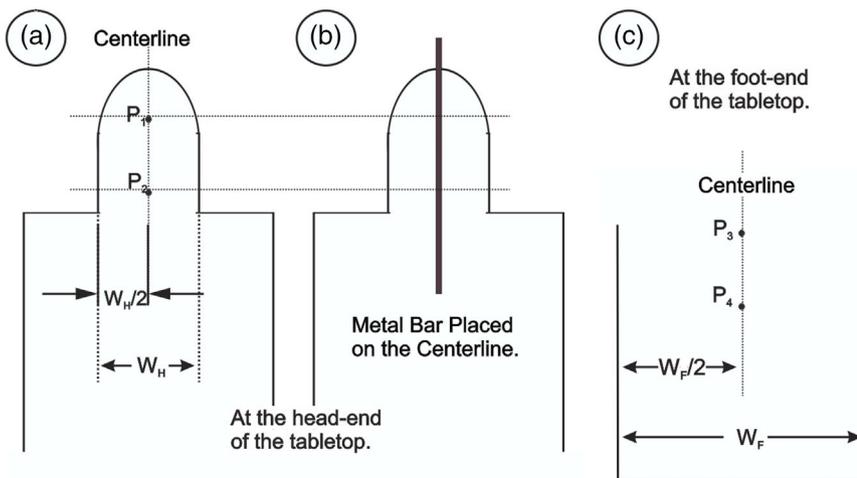

FIGURE 3 Determine the center line. Measure the width "W" of the tabletop at the head end at two locations, say 20 cm apart. Mark the center points P_1 and P_2 and draw a straight line. Similarly, connect center points P_3 and P_4 and draw a straight line. (Alternatively, draw a straight line connecting P_1 and P_4). Therefore, P_1, P_2, P_3, and P_4 are on one straight line running entire length of the examination tabletop

in X- and Y-directions with the exception in the Z-direction.

5. Move the tabletop in the positive Z-direction until the tip of the metal bar placed on the tabletop gently touches the gantry. The table location is at $(X,Y,Z) = (0,0,Z_{HMax})$. Z_{HMax} signifies the tabletop is at the furthest extent of the Z-axis at the head-end. The tip of the metal bar should be pointing to the central axis of rotation, that is, the mechanical rotation axis of the gantry. Using the laser as a guide, mark a sign indicating the location of the mechanical rotation center of the C-arm. (See Figure 5.)

6. Place a self-leveling crossline laser alignment device at the foot end. The vertical laser beam should be aligned to the centerline of the tabletop.

7. Move the tabletop to the furthest point towards the foot-end $(X,Y,Z) = (0, 0, Z_{FMax})$. Z_{FMax} signifies the tabletop is at the furthest extent of the Z-axis at the foot end (see Appendix E for details). It should be pointed out that a very long stiff bar can be employed in place of the laser alignment device.

This alignment evaluation procedure may be modified appropriately to match the mechanical configuration of the system such as a ceiling-suspended C-arm or ceiling-suspended tabletop.

2.1.2 | Alignment of the lateral plane (B-plane) with the C-arm and examination table

- For a biplane system, the lateral plane may be locked at 90° to the A-plane at $(X,Y,Z) = (0,0,Z)$. Rotate the entire system (both A- and B-planes together), and observe in both display monitors that the metal bar is located in the middle of images from both planes.
- Depending on the mechanical configuration of the system, the ceiling-suspended C-arm (often refer to as L-arm due to its shape) may be designed to function as a second primary positioner and can be employed in tandem with the main primary positioner. In these systems, the centerlines of both the A- and
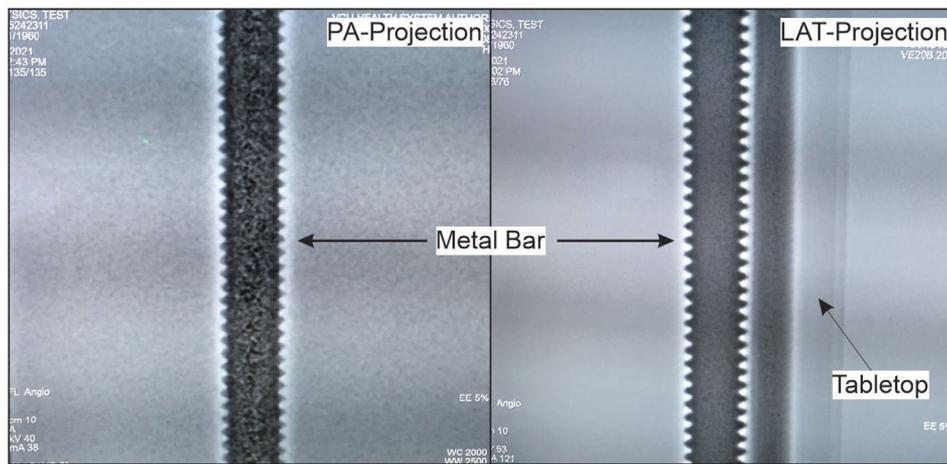
FIGURE 4 Photographs of the display monitor showing the metal bar is in the middle of the image (in PA projection on the left) and rotated 90° (in LAT projection)
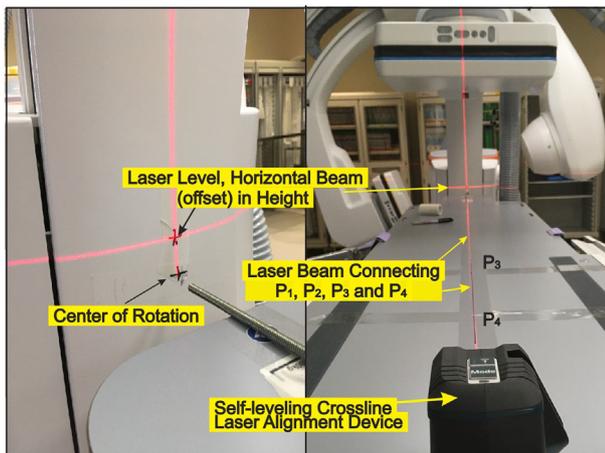

FIGURE 5 On the left, the metal bar is pointing to the center of mechanical rotation. The crosshair of the laser beam is offset in height due to the self-leveling laser beam of 40 mm from the tabletop surface. Note that the vertical laser beam is connecting all measurement points P_1, P_2, P_3, and P_4 running through the centerline of the tabletop

B-planes should be aligned such that the metal bar appears as shown in Figure 4 for the A-plane. For the B-plane, as an LAT projection in PA projection geometry, the image will be displayed horizontally. However, the image of the B-plane may be rotated 90° and displayed vertically similar to A-plane is presented. Then, the metal bar will appear as one contiguous bar across two monitors.

Note that the X-ray tube assembly is commonly installed on the right side of the patient in cardiac catheterization systems to minimize geometric magnification of the heart. Conversely, the X-ray tube assembly is installed on the left side of the patient in neurologic and visceral angiography systems so that the fluoroscopist receives less scattered radiation. For biplane neurologic and visceral systems, the installation configuration of the X-ray tube and the image receptor is reversed. Because the anatomy of interest is either centrally located or spread over the length of the body, it is advantageous to install the imaging chain in such a way as to minimize scattered radiation to the fluoroscopist.

NOTE 2: There are biplane IXE systems in which the lateral plane can be mechanically flipped/rotated about the Y-axis to accommodate the clinical needs of all cardiovascular interventional examinations.

2.1.3 | Verification of the proper functioning of mechanical parts and safety mechanisms

All mechanical parts should be evaluated to ensure that they operate smoothly over the entire range described in the installation drawings and to ensure that any installed detents and locks are functioning properly.

- Typically, the C-arm (A-plane positioner) is equipped with primary and secondary axes (as shown in Figure 2). The range and accuracy of available angulation depend on the configuration of the X-ray tube assembly and the primary imaging axis. The collision avoidance safety switches must be tested during both single-plane operation and biplane operation. For a ceiling-suspended single-plane system, the entire movable range of the C-arm should be tested on both sides of the examination table.
- The L-arm (B-plane positioner) is equipped with angulation capabilities corresponding to the primary axis of rotation (as shown in Figure 2a) and rotation of the L-arm as a whole about the Y-axis. If the L-arm can be flipped, the coordinates and signs displayed ($+X$

and −*X*) should be carefully recorded for application and/or correction for peak PSD calculations.

- Depending on the design of the system, the table-top may offer various motions in linear translation and rotation about all three axes. All available table motions and locks should be tested for proper function.
- The video display monitor(s) (large format or multiple monitor assembly) must be assessed to ensure that the monitor(s) can be moved without too much effort and that the range of motion allows for proper viewing from either side of the examination table. When stationary, the entire assembly should not sag down or rotate and should remain stationary yet allow for easy movement.
- Any ancillary equipment installed on overhead arm(s) (e.g., surgical lights, power injector) must be evaluated to ensure that it can be easily moved and yet remain stationary when released.
- Protective radiation shields must be installed such that they are within the active range of motion of the fluoroscopists, can be employed from either side of the examination table (if so designed), and will remain in a fixed position without movement or sagging when released.
- Proper functioning of the 5-min cumulative imaging time warning alarm must be verified

2.2 | X-ray generator and radiological parameter accuracy

Radiological exposure parameters can be easily measured with most commercially available solid-state detector systems (SSDS). Detailed instructions regarding the operation of these detector-electrometer systems are provided by the manufacturers.

Note that for many IXE systems in clinical operating modes, X-ray generator parameter settings are under the control of the automatic dose rate control (ADRC) system, and the end user may not be able to manually set parameters. For acceptance testing, generator parameter tests should be conducted within service mode to gain control of these radiographic parameters. If the physicist is not familiar with service mode, the service (or installation) engineer from the specific vendor should be asked to assist.

During these test procedures, the image intensifier (II) or the flat panel image receptor (FPIR) should be protected from excessive radiation unless the logic of ADRC mode is an essential part of the testing. A piece of lead at least 1/8 inch (3 mm) thick should be used to cover the II or the FPIR. A specially designed protective piece may be available from the manufacturer for this purpose.

A typical experimental setup is depicted in Figure 6. Note that, for consistency, the SSDS is positioned PERP

(see NOTE 3A), and the SID is set to the maximum available distance for the imaging system. Manufacturers can specify an alternate position for the PERP, so the operator's manual should be consulted.

> **NOTE 3A**: The term "interventional reference point" (IRP) has been renamed by the IEC as "PERP" (IEC 60601-2-43).[2] "PERP" is also used in International Commission on Radiological Protection (ICRP) reports and on the International Atomic Energy Agency (IAEA) website.

> **NOTE 3B**: To be consistent with IEC 60601-2-43[2] and National Council on Radiation Protection and Measurements (NCRP) Report No. 168, the SID is defined as the source-to-image **receptor housing** distance rather than the source-to-**image receptor flat panel** distance (Figure 6).

To evaluate the radiological parameters described in the following sections, it is best to use manual mode unless physics mode or user QC mode is provided within the end-user mode, as specified in NEMA XR 27–2013 standards and guideline publications.[1]

2.2.1 | Tube potential (kV)

For guidance regarding the assessment of tube potential in **fluoroscopy mode**, see Appendix A, "Fluoroscopy Tube Potential Accuracy." For guidance regarding the assessment of tube potential in **acquisition mode,** see Appendix A, "Acquisition Mode." For these evaluations, an accuracy of at least ±5% is expected; alternatively, consult the manufacturer specifications.

> **NOTE 4A**: Although accuracy better than ±5% can be attained, some state regulatory agencies specify that ±10% accuracy is acceptable.

> **NOTE 4B**: It may seem redundant to assess tube potential accuracy with both fluoroscopy and acquisition modes. However, tube current loading is substantially different between the two operations. Thus, at the time of acceptance testing, tube potential should be measured using both modes.

2.2.2 | Tube current-time product (mAs) and output linearity

Tests for tube current-time product and mA linearity are accomplished concurrently; see Appendix A, "Acquisition Mode." The output linearity over the available tube potential range is evaluated with the small focal spot set at, for example, 40 mA and 100 ms (4 mAs) exposure, and the large focal spot set at, for example, 200 mA and
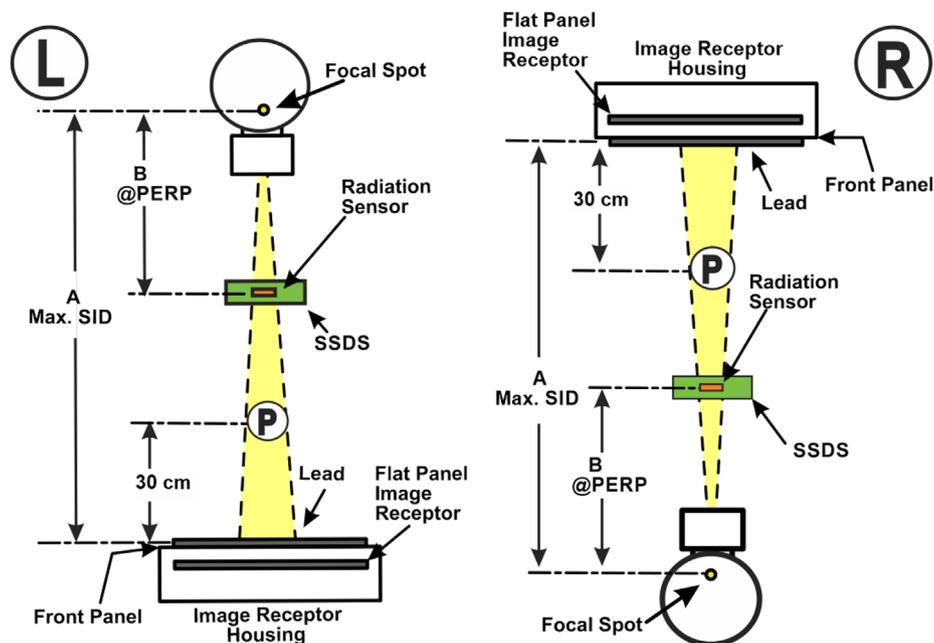
FIGURE 6 Experimental setup for measuring radiological parameters. The radiation sensor in the SSDS is located at the PERP, which is typically 15 cm from the isocenter toward the X-ray source. Depicted on the left is the anteroposterior-projection geometry, which is obtained by flipping the primary gantry C-arm 180° from its normal position. On the right, the SSDS is turned upside down to face the X-ray source. Without this setup, the attenuation caused by the examination table could alter the measured values. The support table (described in Appendix C) is needed to keep the SSDS at the PERP. The table has an opening in the middle so that no tabletop or patient comfort mattress is located in the primary radiation beam. Alternatively, this geometry can be reproduced by rotating the C-arm to the lateral position to avoid effects from the tabletop. The location "P" is the patient entrance exposure measurement point, 30 cm from the image receptor front face plate

200 ms (40 mAs). In this case, the output measured will have a ratio of 4 mAs: 40 mAs (1:10). Note that the regulatory requirement for output linearity is applied to two successive mAs stations, not two different focal spots. As shown in Appendix A, item 5, the output linearity should show a tolerance better than ±10% based on the state regulation, although, ±5% is achievable.

The radiation output linearity is evaluated as depicted in Appendix A, item 7. The average ratios of mGy/mAs obtained at any two consecutive mAs selector settings typically do not differ by more than 10% of their sum for radiographic equipment.

2.2.3 | Pulse width and pulse rate

In general, exposure time is one of the most accurately controlled parameters in a fluoroscopic system and can be easily measured with noninvasive SSDS. Pulse width of greater than 10 ms may be measured with SSDS as a single exposure or as a train of pulses with varying pulse widths and pulse rates. In Appendix A, item 2, exposure times of 100 and 200 ms are evaluated, with the results shown in item 4.

For pulse widths less than 10 ms, the temporal resolution limitation of most SSDS will result in significant inaccuracies. Alternatively, the pulse width can be accurately

measured semi-invasively by connecting a storage oscilloscope to the kV test point within the generator control cabinet. Those who are not familiar with semi-invasive and/or invasive testing should request assistance of the service engineers. (The use of test points in the generator control circuit is described in Appendix B).

Commonly employed clinical pulse rates (frames/s) should also be measured for accuracy. Most SSDS are capable of displaying pulse rate; alternatively, the previously mentioned oscilloscope can be used. However, most SSDS connected to a laptop computer or proprietary display unit are capable of showing the pulses in graphics or in a display window; thus, the pulse rate can be easily determined.

2.2.4 | Tube current (mA)

Measurement of the tube current is no longer considered necessary with the use of inverter-type high-frequency generators, as these generators have a built-in high-voltage divider and are self-calibrated. However, the tube current can be measured indirectly using the output linearity to obtain the relative mA values. In the example described in Section 2.2.2, the exposure time was shown to be accurate, with a ratio of 10:1 in mAs between the two focal spot settings.

Therefore, a tube current ratio of 5:1 is expected and is seen with this example using 40 and 200 mA. However, only the linearity is verified with this technique, not the actual tube current value.

A commercially available clamp-on, induction-type current measurement probe (mA probe) can be used to measure current noninvasively. Using this mA probe at the X-ray tube end of the high-tension cable is the preferred method for measuring current; however, this requires disassembly of the protective shell covering the X-ray tube assembly, as the cables are normally installed such that there is no room to accept the mA probe.

If direct measurement of the tube current is necessary, the measurement can be performed at the high-tension transformer end of the high-tension cable. This requires opening the generator/transformer cabinet and locating the anode side of the high-tension cable. Once again, those who are not familiar with semi-invasive and/or invasive testing should request assistance of the service engineers. In general, however, tube current measurement is not recommended or necessary for the reasons stated above.

2.2.5 | First HVL

Single-shot HVL values measured and calculated with an SSDS system are generally acceptable and may be used in lieu of those obtained with the traditional method using an ionization chamber and Type 1100 aluminum (Al) sheets specified by the FDA. To meet the IEC standard, sheets of 99.9% pure Al must be used. However, an SSDS HVL measurement is quicker and easier to obtain, especially on imaging equipment for which direct control of generator parameters is not possible. If there are doubts about an SSDS HVL measurement, or if the measured value does not meet or is close but not meeting the FDA specified value, confirmation of the SSDS value using the traditional method is recommended. Sample test results for HVL are depicted in Appendix A, item 6. For equipment manufactured after June 10, 2006, regulations specify that the HVL must be at least 2.9 mm Al at 80 kV, for example.[4]

Note that the HVL should be measured using the imaging mode and protocol with the least amount of added filtration (zero-added filtration is preferred). If this information is not available, the IXE manufacturer should be contacted to ensure that the minimum HVL measured is valid for any of the imaging conditions available.

2.2.6 | Total filtration (mm Al)

When using SSDS, the total filtration displayed by the SSDS is a calculated value. The total filtration results should be consistent (within ±0.5 mm) over the entire range of tube potentials employed in diagnostic radiol-ogy. The total filtration is, in general, a "free" measurement when using an SSDS; this parameter is often a provided output that can be recorded or compared, but no regulations or validity assessments regarding total filtration are available.

2.3 | Radiation output measurements and SID tracking of ADRC

Once generator-related tests are completed, the X-ray imaging system should be brought back to the clinical mode of operation so that ADRC is in full operation, simulating actual clinical conditions.

Radiation output is typically evaluated under two different arrangements; those tests for maximum air kerma rate (AKR) and those that are geared toward assessment of the automatic dose control logic.

2.3.1 | Maximum air kerma rate

The FDA's maximum AKR limits are described as measured free-in-air, without the contribution of any scattering medium. The presence of scattered radiation from the table, the table pad, or any added attenuating material such as PMMA is likely to increase the measurement recorded by an ionization chamber or radiation sensor, which could lead to erroneous failing measurements for maximum output. As such, maximum AKR measurements must be performed free-in-air with no additional material in the beam path, with the exception of attenuation material to drive the ADRC to its maximum power loading.

Maximum AKR can be measured using the setup shown in Figure 7. In this setup, the examination table is rotated outside of the beam path. To conform to the free-in-air definition, the ionization chamber or radiation sensor is, in turn, extended off the edge of the examination table and positioned in the primary beam path. Alternatively, if the examination table cannot be moved out of the beam path, the measurement can be obtained with the image chain in a horizontal orientation.

From a regulatory point of view, the maximum radiation output must be verified at both maximum and minimum SIDs; additionally, depending on the measurement geometry, the measured radiation output must be corrected for the location "P," the patient radiation entrance point, 30 cm from the image receptor. The measured maximum radiation AKR must be ≤88 mGy/min under normal operation and ≤176 mGy/min under high-dose rate operation.[5,6] For systems equipped with SID tracking, the maximum output measurements should be conducted at the maximum SID, minimum SID, and at least one additional SID to ensure that the maximum radiation output at location P does not exceed regulatory limit irrespective of the SID.

FIGURE 7 Setup for measuring maximum output. "A" is the source-to-image receptor distance and "B" is the source-to-radiation sensor distance located at the patient entrance exposure reference point. In both geometrical arrangements, the ionization chamber or radiation sensor is mechanically suspended/supported from the examination table at the PERP, whereas the SID is set to the maximum available distance. "P," the patient radiation entrance point (or, the FDA defined patient dose measurement point), is located 30 cm from the image receptor. The attenuation material (lead and/or Cu sheets) can be placed on the image receptor housing in the case of anteroposterior projection, as shown on the left. For ease of setup, we keep measurement system at the PERP; however, the values must be corrected to 30 cm from the receptor. Alternatively, the attenuation material can be suspended from the image receptor housing, as shown on the right
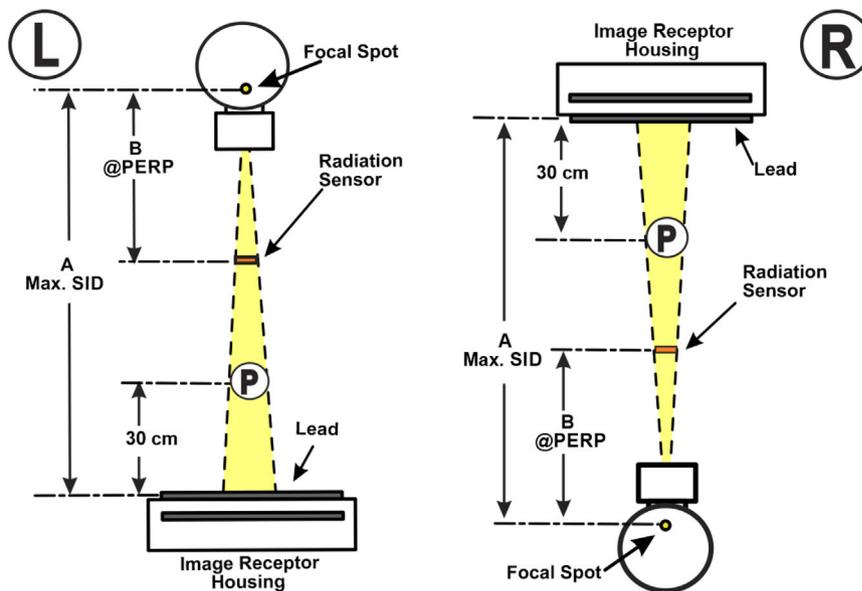
2.3.2 | Assessment of the ADRC

The actual patient entrance air kerma (or AKR) should be measured under more clinically realistic conditions, including automatic dose control logic enabled, normal positioning of the examination table, use of a table pad, and presence of back scatter from any phantom used.

In terms of acceptance testing, this report describes free-in-air AKR measurements using varying thicknesses of PMMA slabs as the attenuation phantom and several pieces of 1-mm-thick Cu sheets.

> **NOTE 5A**: If the fidelity with clinical patient radiation exposure is the primary aim, a radiotransparent ionization chamber can be employed in place of the SSDS that may affect the automatic exposure control. This is especially true if the sensing area(s) for the fluoroscopic automatic control cover the entire image area such that the radiation sensor cannot be positioned outside the sensing area(s). To minimize the influence of the lead backing (~1.0 mm Pb equivalent) of SSDS, the radiation detector/probe should be placed outside of the sensing area(s) for the fluoroscopic automatic control.
>
> **NOTE 5B**: Testing dose rates for recorded/acquisition imaging modes (cine, DSA, roadmap) is problematic because of (a) the exceedingly high dose rates (often >1000 mGy/min) and (b) the absence of regulatory limits on these rates. Care should be taken during these measurements to avoid excess X-ray tube heat loading and possible sensor "burn-in" on the FPIR.

To aid in the following discussion of ADRC measurements, a sample form is provided in Appendix A. This form is based on a cardiovascular system with six field of

views (FOVs), including data at a sample FOV of 32 cm diagonal (item 8). The default FOV for calibration may depend on the size of the installed FPIR. Additionally, various control parameters can affect the radiation output, including the pulse rate, fluoroscopy curve selection, and operation mode (low, normal, or high). The numerous combinations of these factors will result in an enormous amount of data. However, the testing process can be streamlined by consulting the X-ray imaging manufacturer regarding the system's default configuration for calibration. Most likely, a default FOV is selected at the time of calibration, and the data (including the radiation output) are scaled according to the system design. Additionally, when high-output mode is selected, the pulse rate may be increased from, for example, 10 pulses/s (pps) (in low or normal mode) to 15 pps as the system default setup.

Because of these factors, it is advisable to first determine the primary application of the specific IXE system under acceptance testing and the type of procedure for which the system will be employed (e.g., neurological angiography, visceral angiography, and cardiac catheterization). In the selection menu, the most likely applications are shown when the system power is turned on. Because it would be difficult and time-consuming to evaluate every procedure programmed into the system, two or three procedures associated with the systems primary function may be selected for acceptance testing.

The geometry employed for this test is depicted in Figure 8. On the left of Figure 8, the primary plane C-arm (A-plane) is rotated 90° to a lateral projection to support the PMMA plates on the examination table. On the right, a homemade supporting table with an opening in the middle is employed. Although either geometry will work, the geometry using the supporting
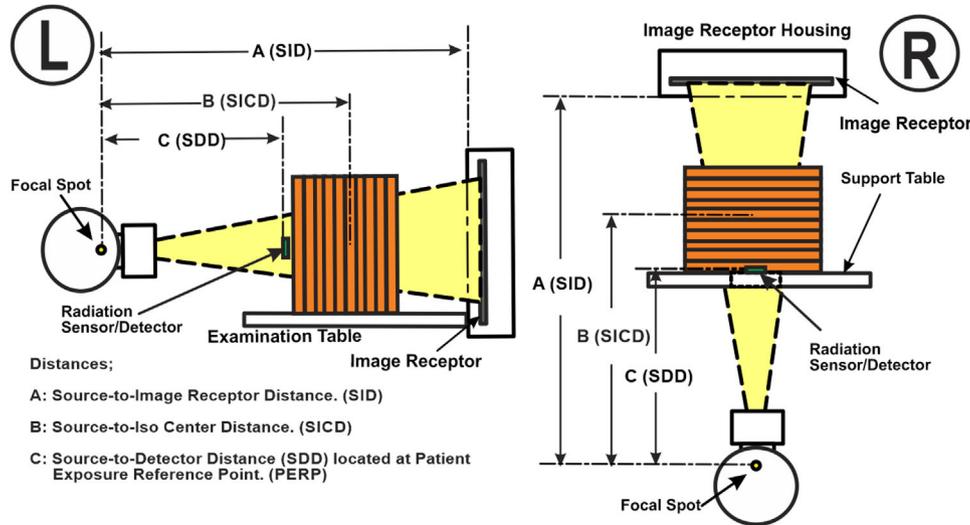
FIGURE 8 Experimental setup for measuring radiation output. In both geometrical arrangements, the tabletop and the table pad are not included in the measurements. The distance "A," the SID, is set to the maximum distance available for consistency. The distance "B" is the source-to-isocenter distance (SICD). The isocenter axis "B" in this example had already been determined mechanically. The source-to-detector distance "C" is located at the PERP for consistency and for convenience in placing the radiation sensor for measurements of patient entrance dose rate. Note that use of an ionization chamber results in increased entrance surface dose rates due to backscatter. This is minimized if the chamber is placed farther from the scattering material by moving PMMA closer to the flat panel image receptor

table is a more convenient option. For institutions with a relatively high number of IXE systems, the supporting table is an invaluable asset as a testing tool, as this table can also be used with mobile C-arm equipment, which may be coupled with a variety of patient tables. A drawing of a sample supporting table is provided in Appendix C.

NOTE 6A: To minimize the influence of a radiation probe on the ADRC, one can simply place the detector outside of the sensing area. Alternatively, the sensing area can be selected from the control console or table-side control box, if available, such that the radiation probe and the sensing area are not superimposed. If the sensing area covers the entire image receptor, the lead-backed SSDS may not be the ideal detector to use. In such a case, an ionization chamber is recommended, with the metalic portion of the ionization chamber (if so designed) placed outside of the FPIR when possible.

NOTE 6B: PMMA is employed extensively in this report. Aluminum and copper sheets are more convenient to transport and may be preferred for annual or periodic evaluation of IXE. It should be noted, however, that the ADRC fluoroscopy curves are designed based on "water equivalent" and/or PMMA to simulate patient attenuation by the major IXE manufacturers whether it is using static or dynamic spectral shaping filters (SSFs). For acceptance testing, the TG strongly recommends PMMA be employed to evaluate the ADRC functionality. Additionally, use of aluminum (or copper) causes the ADRC to oscillate as it attempts to find a stable combination of tube potential, tube current, pulse width, and SSF at certain key calibration points (for example, at attenuation of 18–20 cm water equivalent). This is especially important for IXEs employing dynamic ADRC logic. This will result in an unstable dose rate registered by the radiation detector as has been discussed in AAPM Reports 125 and 190. Thus, TG 272 recommends PMMA be employed for both acceptance testing and annual equipment evaluation of IXE systems. Aluminum and/or copper filters may be utilized when the fidelity of fluoroscopy curves is not the primary concern.

2.3.3 | Radiation output as a function of PMMA thickness

AAPM Report No. 125 established that the use of SSFs is common in high radiation-level fluoroscopy equipment.[7,8] The selection of SSFs is based on the fluoroscopic curves that, in turn, are dependent on the hardware capabilities of the equipment, including the X-ray tube type and generator power rating. However, the applications specialist must assess the default programming of the fluoroscopic curves to determine the image quality preferences of the fluoroscopists involved.

Evaluation of radiation output versus PMMA thickness ensures that the SSFs are functioning and that the data obtained are suitable as a benchmark when assessing the clinical functioning of the equipment in terms of the logic of fluoroscopy curve or trajectory.

2.3.4 | Dose and dose rate at the PERP

The patient entrance exposure with backscatter can be measured at the PERP, as shown in Figure 8, or at any other convenient distance from the X-ray source. Regardless of how the exposure is measured, the geometrical information must be recorded to allow for scaling. Although the PERP dose and dose rate are typically not the same as the patient entrance exposure or patient dose, both are important data points that can be used for patient dose tracking at the PERP and can also be used in conjunction with fluoroscopy patient dose monitoring and tracking software programs.

2.3.5 | Image receptor input dose and input dose rate

FPIR input dose is defined as the radiation that impinges on the image receptor as opposed to the patient; this parameter is thus a better indicator of image quality than PERP. Previous generation of IXE systems used constant input dose (dose rate) logic, in which this report will hereafter refer to as signal-to-noise ratio (SNR)-optimized logic (SNR optimization). The input dose to the FPIR, the fluoroscopy frame dose rate, and the acquisition frame dose rate were previously measured as part of acceptance testing or a study related to SSF.[9]

Over the past few years, the newest IXE systems have been equipped with contrast-to-noise ratio (CNR)-optimized logic (CNR optimization), and the input dose per frame has become a moving target. As the PMMA thickness is changed, the ADRC seeks optimum contrast for each specific condition of attenuation provided by the PMMA. The FPIR input dose will therefore vary to maintain optimum contrast. Thus, FPIR input dose (and input dose rate) must be measured with extreme care. There is no established procedure to properly evaluate the relationship of FPIR input dose (and input dose rate) to image quality on CNR optimized fluoroscopy systems, nor is there a suitable phantom available on the commercial market for image quality assessment.

It is therefore premature, at this time, for TG 272 to address any specific test procedure for evaluation of CNR-optimized fluoroscopy systems. CNR optimization is briefly discussed in Appendix D.

2.3.6 | Displayed patient entrance reference point air kerma verification

The measurement and verification of PERP dose were described in detail in AAPM Report No. 190.[10] This report recommended the use of integral mode to ver-ify the displayed PERP air kerma against the physically measured air kerma with the FOV set to a known area at a known distance from the radiation source. The integral mode is selected to avoid the continuously changing dosimeter reading that occurs with rate mode measurement due to "digital jumping" of the FPIR control circuit. Digital jumping is caused by the operation logic searching for a stable point (of tube potential in particular) on the fluoroscopy curve. This phenomenon is observed with the use of Cu or Al sheets as the attenuation material.

Although the previous report recommended comparing the displayed PERP air kerma with a measurement of integral air kerma, this can also be done by comparing the measured and displayed AKRs (Appendix A, item 11). The rate mode method reduces the need for an additional setup of measuring equipment and may reduce the overall time for the inspection. In-air measurement conditions must be met; hence, no backscatter can contribute to the measurement. If the radiation probe of the SSDS radiation detector is placed at the PERP, the PERP dose and dose rate can be determined. The dose-area product, or the air kerma-area product (KAP), can also be verified if the FOV at the PERP is known.

Going beyond the PERP air kerma, some manufacturers have made use of the knowledge of equipment geometry and radiation output to create real-time dose maps (dose mapping) that can be displayed during a procedure. Although PERP air kerma tallies the total tube output during a procedure, dose maps show the spatial distribution of that tube output on a stylized patient model to aid in spreading radiation skin dose when possible.

The IEC 60601-2-43:2010AMD2 standard published in 2019 standardizes the units of measurement a vendor may choose from to display the radiation quantity of air KAP.[2] Additionally, the tolerance of the KAP accuracy is ± 35%. The three choices are $Gycm^2$,[2] $cGycm^2$ [numerically identical to μGym^2], and $mGycm^2$.[2] However, as this standard applies specifically to fluoroscopes intended for use in fluoroscopically-guided interventions, other types of fluoroscopes are not subject to this standard and may choose other units of measurement for the displayed air KAP.

This same IEC standards also recommend that dose mapping capability should be available as part of the basic safety and essential performance abilities of interventional angiography equipment.[2] The IEC guidance also recommends that the accuracy of any such dose maps should be evaluated during physics testing once standards are established and implemented by various manufacturers. Because standards for dose maps do not currently exist, it is outside of the scope of TG 272 to define appropriate acceptance testing for the accuracy of skin dose maps.

2.4 | Collimator congruence test

The objective of the congruence test is to ensure that the X-ray field is appropriately sized and aligned with the image receptor. Good congruence and correct alignment not only prevent unnecessary exposure to patients but also reduce scattered radiation to medical personnel while improving image quality. To this end, the central ray of the X-ray beam should be aligned with the center of the image receptor to minimize image cutoff and to avoid irradiating tissues that do not contribute to image formation.

2.4.1 | Congruence of radiation field size with the image receptor

Because of potential mechanical sag of the C-arm, the congruence test should be performed using various angulations and rotations of the C-arm with respect to its primary and secondary axes. It must also be conducted on all available FOVs.

Depending on the equipment design, the image receptor may be rotated, with respect to the *Y*-axis as shown in Figure 2, to optimize the imaging area to fit with the positioning and shape of the anatomy. The collimator may then be synchronized with the rotated FPIR to optimize the imaging area available, whether the collimation is rectangular or circular in design. The congruence test should include measurements at the following projections:

- posteroanterior and anteroposterior,
- 45° and 90° right anterior oblique (RAO) and left anterior oblique (LAO), and
- 45° cranial and caudal.

Of the items listed above, the posteroanterior projection is often the only geometry at which the congruence test is performed. For reducing the number of congruence test measurement, the left or RAO may be combined with the cranial or caudal measurements.

Many approaches to congruence testing have been described. For example, a detailed test procedure using a cassette or film is described in AAPM Report No. 74.[11] The congruence test is best performed using a fluorescent screen or radiochromic film and rulers (or plate) with lead markers to identify the radiation field size placed at a distance of the users discretion. Computed radiography cassettes may be used in place of the fluorescent screen for indirect visual verification of the radiation field for all FOVs. Also, there are commercially available, stand-alone digital radiography detectors that work very well for this purpose. There are commercially available devices that retain the detected radiation and use LCD bars or long-latency fluorescent screens to allow for visual verification. With each of these techniques, the physical size of the radiation field can be compared with the image displayed on the monitor (Figure 9).

In the example shown in Figure 9, an attenuator (a lead sheet in this example; ~1/16 inch, 1.56 mm) is attached to the FPIR to drive the X-ray generator to gain sufficient screen brightness for visualization of the radiation field. The fluorescent screen is placed in the primary beam, with lead BB shots employed as the scales (in cm). While stepping on the fluoroscopy exposure pedal, the operator then aligns the fluorescent screen to the FOV (roughly 12 cm × 12 cm in this example), as shown on the left side of Figure 9. The two images are then compared to determine the alignment of the radiation field to the image receptor. The congruence test should show that the radiation field is no larger than 2% of the SID in any direction and no smaller than the FOV of the image receptor active size. The shadow of collimator blades or iris should be confined within the specified FOV.

The simplest congruence test involves ensuring that the collimator blades are just visible within the image field when the collimator is opened to its fullest extent under all FOVs available in the imaging chain. However, the video mask must be deactivated for this test and this test is only valid if the blades are visible. If the individual collimator blade cannot be visualized, further testing is needed to determine the amount of incongruence.

Requirements regarding X-ray field limitations and alignment of fluoroscopic systems are available in the FDA resource manual for compliance test parameters of diagnostic X-ray systems.[12] Specifically, X-ray fields produced by fluoroscopic equipment without an II should not extend beyond the entire visible area of the image receptor; means are provided for stepless adjustment of the field size. The minimum field size at the greatest SID must be ≤5 cm × 5 cm. For fluoroscopic equipment with an II, neither the length nor the width of the X-ray field in the plane of the image receptor should exceed that of the visible area of the image receptor by more than 3% of the SID. The sum of the excess length and the excess width should be no greater than 4% of the SID.

For rectangular X-ray fields used with circular image receptors, the error alignment should be determined along the length and width dimensions of the X-ray field, which pass through the center of the visible area of the image receptor. Means are provided to permit further limitation of the field. For beam-limiting devices manufactured after May 22, 1979, and used in equipment with a variable SID and/or a visible area of >300 cm^2, means are provided for stepless adjustment of the X-ray field.

Equipment with a fixed SID and a visible area of ≤300 cm^2 is provided with either stepless adjustment of the X-ray field or with means to further limit the X-ray field size at the plane of the image receptor to ≤125 cm^2. Stepless adjustment should, at the greatest SID, provide
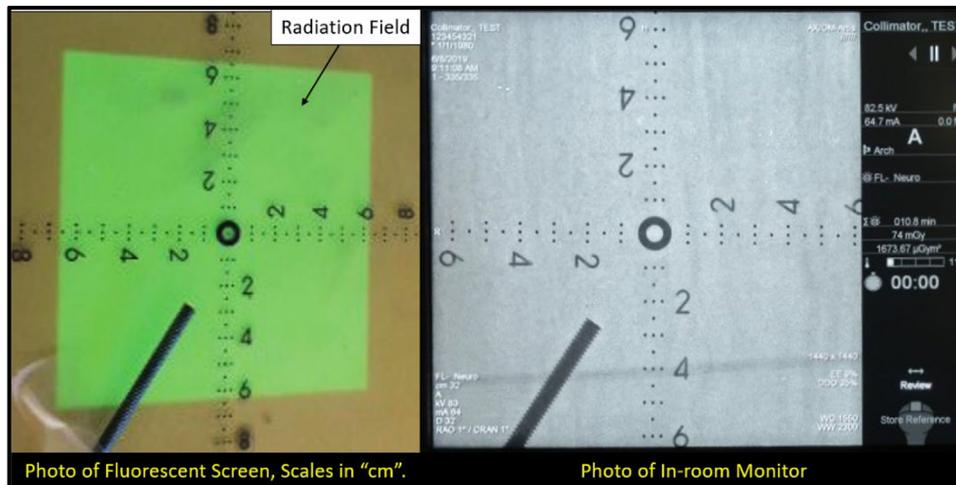
FIGURE 9 Congruence test. The photograph on the left shows a fluorescent screen with rulers using lead dots and lead numbers for field size identification. The last-image-hold fluoroscopy image is shown on the right. By comparing the corresponding four sides of these two images, the congruence of the radiation field to the image receptor can be evaluated with the naked eye

continuous field sizes from the maximum obtainable field size to a field size of ≤ 5 cm $\times$ 5 cm.

2.4.2 | Centering of the central beam to the center of the image receptor

The alignment of the X-ray central beam with the center of the image receptor can be easily confirmed with the use of two metal washers of the same dimension or of a similar size, as described previously.[13] A simplified method is provided here: using two metal washers of identical size, place one washer on the tabletop, and attach the other to the center of the FPIR (see left side of Figure 10). Pan the examination tabletop to align these two washers under a geometry of approximately 2× magnification with the smallest FOV available. If the radiation beam is centered with the center of the FPIR, an image similar to that shown on the right side of Figure 10 should be observed. In addition, if the X-ray tube (insert) or the tabletop is not perpendicular to the image receptor, the washer placed on the tabletop will appear as an elongated ring, whereas the washer attached to the FPIR will appear as a normal ring.

2.5 | Display monitors

Fluoroscopy display monitors installed for IXE systems are a critical part of the imaging chain. The images displayed on the monitors for these systems are used to make clinical diagnoses and to guide the placement of needles, catheters, or other devices inside the body, whereas modality monitors for other types of imaging are primarily used for quality assurance of images

before the images are sent to higher performance diagnostic displays. Additionally, fluoroscopic monitors are often used in brightly lit suites with high ambient lighting, which can have negative consequences on image quality. Thus, care must be taken to ensure the consistent display of images.

The reader is referred to AAPM TG Report No. 270[14] and its associated update[15] for a full discussion of display characteristics. TG Report No. 270 recommends measuring several key display characteristics, including minimum/maximum luminance, luminance response, and luminance uniformity; these characteristics will be briefly discussed here. The American College of Radiology (ACR)-AAPM-Society for Imaging Informatics in Medicine Technical Standard for Electronic Practice of Medical Imaging can also be referenced for further information.[16] Although this report is not as detailed as the TG report, its recommendations largely mirror those provided in the TG report and are likely to be updated more frequently.

Fluoroscopy-guided imaging (FGI) systems typically include multiple monitors located in the control room and in the FGI suite itself. For acceptance testing, the following evaluations should be performed for all monitors associated with a system to ensure consistent image presentation.

2.5.1 | Minimum/maximum luminance and luminance ratio

The initial configuration of display operating levels should be based on the ambient luminance (L_{amb}), which is the ambient light reflected from the surface of the monitor. Ambient luminance can be measured
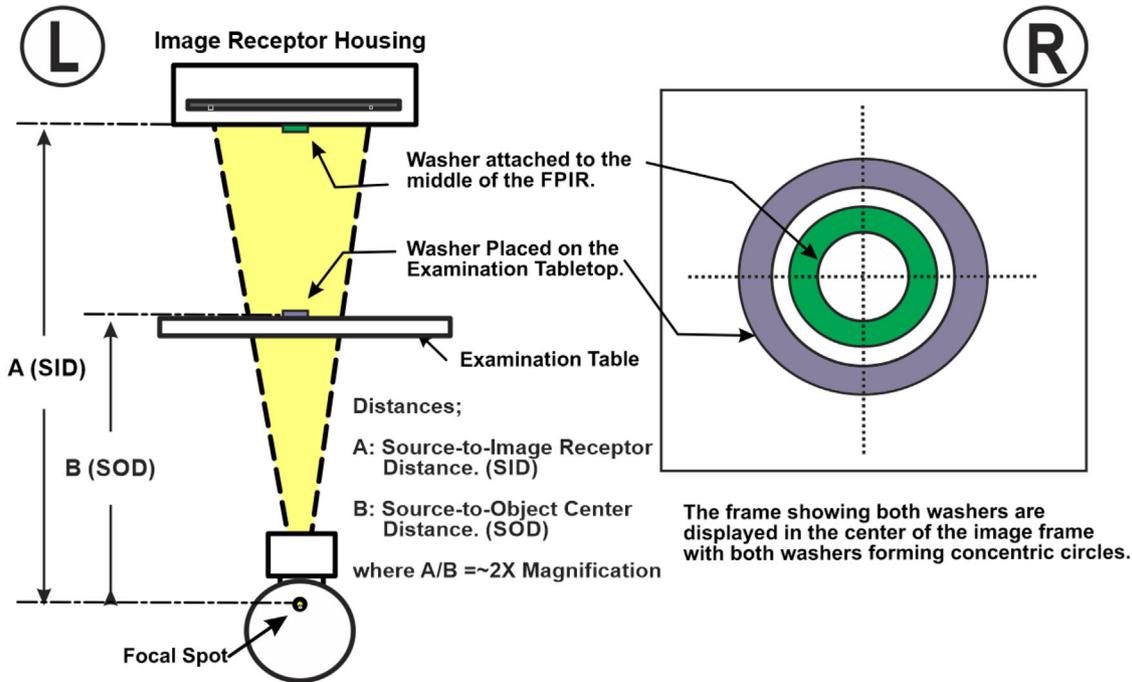
FIGURE 10 Evaluation of radiation beam centering with the FPIR. By using the smallest FOV available, a more accurate centering alignment evaluation can be attained compared to a larger FOV. When the centering is set up correctly, the centers of the metallic washers should form concentric circles in the middle of the image displayed on the monitor

directly with a light meter or can be estimated based on the ambient illuminance and diffuse reflection coefficient (R_d) of the monitor. A recent study found an average R_d of 0.0038 cd/m^2 per lux in a sample of large-format displays used with modern FGI equipment.[17] The display's minimum luminance (L_{min}) should ideally be set such that the ambience ratio (AR, defined as L_{amb}/L_{min} is < 1/4. Once L_{min} is set, the total minimum combined luminance (L'_{min}) can be calculated by summing L_{min} and L_{amb}. The maximum luminance (L_{max}) can then be set, targeting an overall luminance ratio (LR) of 350, with LRs between 250 and 450 deemed acceptable. Note that LR is defined as L'_{max}/L'_{min}, where L'_{max} is the total maximum combined luminance. Note also that on many fluoroscopic displays, options for independent adjustment of L_{min} and L_{max} are limited.

Although the TG 270 recommendations for AR and LR are typically easily achievable in dimly lit reading rooms, maintaining the recommended AR and LR may be unachievable in the brighter environments typical of many FGI suites, leading to loss of image contrast in darker regions of the image. In cases of high ambient illuminance, increasing L_{min} in an attempt to maintain an AR ratio < 1/4 if L_{max} cannot be set high enough to maintain an acceptable LR is not recommended. Increasing L_{min} could cause a loss of available contrast if room lighting is later dimmed. Differing ambient light preferences among operators must also

be considered. In these cases, consultation with physicians regarding the clinical acceptability of the loss of low luminance contrast is advised. In addition, test patterns such as AAPM TG18-AD or TG270-pQC can be useful for evaluating the effects of ambient lighting on low-contrast detectability.[18] If such loss of low-contrast information is clinically unacceptable, possible solutions include dimming the room lights, repositioning monitors to reduce ambient reflection, or replacing monitors with higher L_{max} models.

2.5.2 | Luminance response

TG Report No. 270 also recommends evaluating the luminance response of display monitors. The luminance response describes the relationship between individual gray levels for L_{min} and L_{max}; proper calibration ensures adequate image contrast across the range of displayed values. The DICOM grayscale standard display function has been widely adopted in medical imaging and is recommended.[19] Depending on the test patterns available, users may be able to test luminance response compliance using the 18-point or 11-point response methods described in TG Report No. 270. Deviation of <20% from the DICOM grayscale standard display function is recommended.

In the absence of quantitative assessment of DICOM grayscale standard display function compliance,

qualitative evaluation via test patterns may be used instead. Many test patterns are available for this purpose, the most prevalent of which is the Society of Motion Picture and Television Engineers pattern (SMPTE)[20] that provides multiple grayscale levels and high- and low-contrast objects. However, it should be noted that this pattern was designed to test properties of older cathode-ray tube displays; because of grayscale insensitivity, this pattern is recommended for use with modern flat-panel displays only if no other patterns are available. TG Report No. 270 includes the TG270-sQC and TG270-pQC test patterns, both of which provide objects to better test the luminance response across the entire luminance range of a flat-panel display. If the TG270 test patterns are unavailable or unable to be loaded, the AAPM TG18-QC or TG18-OIQ test patterns are recommended over the Society of Motion Picture and Television Engineers pattern. Any pattern should be evaluated at typical viewing distances and in typical ambient lighting conditions. Readers are directed to TG Report No. 270 for more in-depth discussion regarding qualitative test patterns and suggested pass/fail criteria.

2.5.3 | Luminance uniformity

Luminance uniformity describes the variation in luminance output across the display area. TG Report No. 270 recommends that users primarily focus on qualitative evaluation of local nonuniformities rather than on global quantitative uniformity, although for acceptance testing of new monitors, quantitative methods are recommended. TG Report No. 270 introduced the luminance uniformity deviation from the median (LUDM) metric, which is easily calculated using standard photometer measurements from nine locations on a uniform field. For cases in which a uniform test pattern is not available, simple window width and leveling to produce a uniform display output can suffice. Displays with an LUDM > 30% should be considered for replacement, and an LUDM > 15% should be investigated for possible clinical effects.

Note that many large-format monitors commonly used in FGI can be customized for various arrangements of displayed images. For the purpose of luminance uniformity or test pattern observation, the most common configuration should be used, as attempting to test all possible arrangements of displays from all possible video input devices may not be practical. Also note that many displays include protective covers that may be in place during clinical use; these covers may alter the reflective or transmission properties of the displays. Display testing conditions should therefore mirror clinical operating conditions if protective covers are in place during clinical use.

2.6 | Fluoroscopic dose monitoring and tracking

For patient procedures, recording of the air KAP or the air kerma at the PERP ($K_{air,PERP}$) is required by the Joint Commission,[21] not only to maintain a record of the fluoroscopy dose but also to track the total accumulated dose to assess potential skin injuries. Enterprise-wide radiation dose index monitoring systems (RDIM) software[22] makes compliance with this Joint Commission requirement much more efficient and effective. It is not within the scope of TG 272 to discuss the pros and cons of specific RDIM programs. However, regardless of the program used, key physics corrections must be applied to estimate the PSD as accurately as possible. These key physics corrections must be applied to every event of fluoroscopic exposures in addition to the acquisition exposures. Note that because the exposure events in an IXE study, it can include hundreds of event entries. A RDIM program is an essential tool in this process; application of these correction factors is time-consuming if calculations are performed manually.

NOTE 7: It is noteworthy to point out that, in the July 2021 issue of the Joint Commission Perspectives, the sentinel event definition and chapter have been revised.[23] For a broader scope of radiation injury and dosimetry, readers are directed to National Council on Radiation Protection and Measurements (NCRP) Report No.168, Radiation dose management for fluoroscopically guided interventional medical procedures.[24]

To apply these corrections, the four values described in the following sections may be acquired at the time of acceptance testing. Additionally, further details regarding these parameters for calculating PSD, including the addition of a composite factor that includes back scatter factor (BSF), can be found in a report by DeLorenzo et al.[25] This paper also discusses methods for developing fitting equations for various fluoroscopes.

NOTE 8A: RDIM programs available on the commercial market vary in their level of sophistication and may or may not include the essential corrections required to accurately estimate PSD. The corrections described in Sections 2.6.1 and 2.6.2 are typically not built into the current generation of RDIM programs; manual intervention is therefore required to apply these corrections. In the future, perhaps, these corrections will be built into these programs.

NOTE 8B: Additionally, NEMA XR-27 standards[1] provide TG 190 correction (see Section 2.6.1 below), in the DICOM header so that the correction factor can be read by RDIM programs.

2.6.1 | TG 190 dose correction/calibration (C_{TG190})

The correction factor obtained from the dose-rate mode or the integral dose (as described in Section 2.3.6) is needed to correct the displayed PERP dose (D_{PERP}) to the externally measured dose ($D_{MEASURED}$). The dose correction factor (C_{TG190}) is defined as:

$$C_{TG190} = D_{MEASURED}/D_{PERP}. \tag{1}$$

Empirically speaking, D_{PERP} is often higher than $D_{MEASURED}$ for most systems; thus, C_{TG190} is usually < 1. Values less than 1 provide a margin of safety, and will alert fluoroscopists earlier. The IEC standards allow for a tolerance of 35% in the accuracy of the reported D_{PERP},[26] but 10% to 15% ($C_{TG190} = 0.87$–0.91) over-reporting is usually observed.

2.6.2 | Examination table/mattress attenuation correction (C_{Table} and $C_{Mattress}$)

To more accurately assess PSD, the attenuation caused by the presence of the fluoroscopic examination table-top (C_{Table}) and the patient mattress ($C_{Mattress}$) must be measured. The total correction ($C_{Table\_Mattress}$) is the product of C_{Table} and $C_{Mattress}$ and can range from 0.6 to 0.75 depending on the tube potential (kV), the SSF, and the beam quality (e.g., mm Cu, mm Al).[27] Hence,

$$C_{Table\_Mattress} = C_{Table} \times C_{Mattress}. \tag{2}$$

For accurate patient dose assessment, $C_{Table\_Mattress}$ should be measured with the examination tabletop and the mattress initially as delivered and remeasured when either the tabletop or the mattress is replaced.

The total manual correction (C_{Total_Manual}) that can be predetermined at the time of acceptance testing is therefore:

$$C_{Total\_Manual} = C_{TG190} \times C_{Table\_Mattress}$$
$$= C_{TG190} \times C_{Table} \times C_{Mattress}. \tag{3}$$

Note that Equation (3) is correct only when the X-ray beam is in the posteroanterior projection. Different corrections must be applied when the projection is oblique, lateral, or anteroposterior.

Depicted in Figure 11 is the test geometry for measuring the attenuation of the examination tabletop and mattress. This geometry is similar to the narrow-beam geometry described in the American Society for Testing and Materials International designation F3094-14.[28] However, the geometry shown here has been modified to meet the constraints of typical IXE equipment. Because
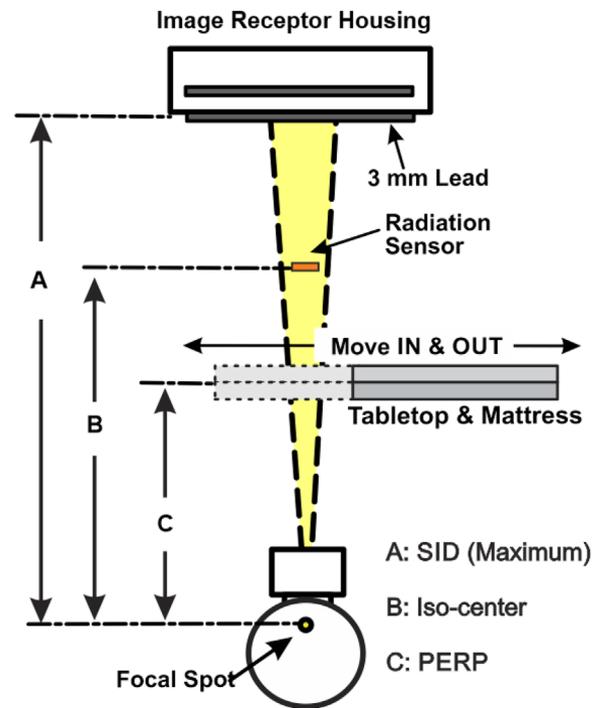
FIGURE 11 Geometry for measuring the transmission ratio (T_R) of the patient examination table and mattress. For measurements of air kerma dose for this T_R calculation, the in-air dose (D_{air}) is measured in the absence of the examination table and mattress (moved out). D_{Table} is measured in the presence of the examination table, and $D_{Mattress}$ is measured in the presence of the mattress (moved in). $D_{Table\_Mattress}$ is measured with both the examination table and the patient mattress in the primary radiation beam

IXE systems employ SSFs whether using the dynamic filter selection of the Seissl method[29] or traditional static filter selection, radiation beam qualities encountered in IXE systems should be evaluated along with the varying tube potential.

The transmission ratio ($T_{R[Table\_Mattress]}$) or correction factor ($C_{Table\_Mattress}$) is defined as:

$$T_{R(Table\_Mattress)} = C_{Table\_Mattress}$$
$$= D_{Table\_Mattress}/D_{air}. \tag{4}$$

And similarly:

$$T_{R(Table)} = C_{Table} = D_{Table}/D_{air}, \tag{5}$$

$$T_{R(Mattress)} = C_{Mattress} = D_{Mattress}/D_{air}, \tag{6}$$

where $D_{Table\_Mattress}$ is the air kerma measured with the examination table and the mattress together in the beam. D_{Table} and $D_{Mattress}$ are the air kerma values measured in the presence of the table or mattress, respectively. D_{air} is the air kerma measured in air with both the examination table and the mattress positioned at least

TABLE 1 Correction factors for T_R through table and mattress

		Tube potential (kVp)							
		60	70	80	90	100	110	120	Average
SSF (mmCu)	0	0.587	0.611	0.628	0.64	0.653	0.661	0.669	0.635
	0.1	0.635	0.659	0.675	0.683	0.691	0.699	0.704	0.678
	0.2	0.651	0.676	0.687	0.697	0.704	0.711	0.715	0.691
	0.3	0.657	0.684	0.697	0.707	0.713	0.719	0.722	0.7
	0.6	0.679	0.701	0.711	0.718	0.723	0.729	0.732	0.713
	0.9	0.692	0.708	0.726	0.723	0.729	0.733	0.736	0.721
	Average	0.65	0.673	0.688	0.695	0.702	0.709	0.713	

50 cm from the primary beam (or as far from the beam as the mechanical configuration of the IXE system allows). Thus, the total $T_{R(Table\_Mattress)}$ is defined as:

$$T_{R(Table\_Mattress)} = T_{R(Table)} \times T_{R(Mattress)}$$

$$= C_{Table} \times C_{Mattress}$$

$$= C_{Table\_Mattress}. \qquad (7)$$

For this assessment, the radiation field size is set to 10 cm × 10 cm at the radiation probe to simulate typical clinical conditions. T_R is most easily measured using the service mode or the end-user measurement mode (physics mode) if available. If the service mode cannot be accessed, the automatic feature must be locked to obtain meaningful measurements. The technique lock feature of the ADRC must be employed, in effect, to disable, the ADRC temporarily after the desired combination of tube potential and SSF is achieved.

A selection of sample data obtained from an IXE system is shown in Table 1. Measurement of T_R was performed on 14 IXE systems using the Seissl method of filter selection. The values listed are typical but do vary with changes in imaging equipment or patient mattress.

Correction of the PSD calculation can be simplified by selecting the most typical combinations of tube potential and SSF (gray cells in Table 1). When only one correction factor can be applied, based on Table 1, a correction of ($T_R =$) 0.7 is suggested for the beam quality correction.[25] It should be noted that T_R is also a function of $T_R = T_R (X, Y, Z, \theta, \varphi)$ where θ is the primary rotation angle and φ is the secondary rotation angle of the C-arm.

2.6.3 | Geometrical correction (C_{Geo})

To more accurately assess PSD, a geometrical correction is required to account for panning of the patient in 3D orientation. Without an RDIM program, this task cannot be easily accomplished. In practical terms, the table up-and-down correction C_{Geo-Y} may be similar for

all events if the table height is kept more or less at a given location for the duration of a case.

Similar to T_R, C_{Geo} is also a function of the geometry employed. Thus, $C_{Geo} = C_{Geo} (X, Y, Z, \theta, \varphi)$. Although the application of C_{Geo} is a straightforward correction, the process can be tedious, as the exposure event can include hundreds of occurrences. C_{Geo} corrections should be applied to all events.

2.6.4 | FOV correction (C_{FOV})

Even if tabletop panning is minimal and the radiation beam entrance point remains the same, the FOV may be as large as 30 cm × 30 cm at the beginning of the examination and collimated to 10 cm × 10 cm for most of the examination duration. An FOV correction (C_{FOV}) may need to be applied in conjunction with C_{Geo}, and $C_{Table\_Mattress}$ may also need to be included depending on whether the angles (θ, φ) caused the primary radiation beam to traverse the table.

2.7 | Image quality assessment

With the advent of new imaging technology such as modern fluoroscopy curve programming and image processing that can be applied both during and after image acquisition, a more rigorous approach to image quality assessment is necessary.

Physical parameters such as input dose rate to the image receptor, SNR, and CNR are of great interest when characterizing the imaging chain, but from a practical and clinical point of view, these parameters are more suitable for troubleshooting image quality problems.

Image quality assessment on fluoroscopes poses a substantial challenge for several reasons. First, there are multiple operational modes that can and should be tested, including multiple dose levels of fluoroscopy and various subtypes of acquisitions such as cine, DSA, single-shot images, and cone-beam rotational acquisitions. Second, clinical images are viewed live, and processing often involves frame averaging from

multiple images. Viewing single fluoroscopic or acquisition images can provide insight into image quality but does not test the full clinical use of the system. Dynamic live image assessment is needed, although equipment may not have the capability to easily store and review sequences of fluoroscopic images for quality evaluation purposes. Third, the type of image that is provided for analysis of image quality may affect the assessment. Often, only "for presentation" image types are available, and these images have already been processed or manipulated. Optimally, following the guidelines proposed in NEMA standard XR 27–2013 will result in "for processing" images that have not undergone image manipulations other than detector uniformity corrections.[1] Finally, many of the image quality metrics may not have benchmarks or passing values, so it is imperative to check vendor literature for guidance. Benchmarks can also be established at acceptance testing, and trends can be monitored or compared from year to year.

Although the above reasons are hurdles to assessing image quality on fluoroscopes, the real challenge lies in understanding how the image formation and dose logic operation function. Without some knowledge from the vendor, image quality assessment is a daunting task. Many vendors perform localized processing within each image or frequency-based filtering such that a traditional test object will confound the system or at least not provide useful information.[30]

The following sections describe the tools used for testing image quality, the methods and rationale for some of the tests that use these tools, and examples of recording methodology and QC that should be considered during acceptance testing and during monitoring of system performance thereafter. Note that many of the tests described may not have pass/fail criteria but should provide useful information regarding how the system operates and serve as reference information from year to year. Sample results from some of these tests may be found in Appendix A. Finally, any thorough image quality evaluation must also be accompanied by dose analysis.

2.7.1 | Phantoms

Several types of phantoms are available for routine QC testing and acceptance testing. Note that the vendor may require the use of a specific phantom for routine physics testing or continual QC.

One type of phantom used for image assessment consists of simple sheets of Cu or PMMA. This type of phantom can be used alone to identify artifacts or nonuniformities in the image or can be used in conjunction with other image quality phantoms to drive the fluoroscopy equipment to clinical levels of operation. Some manufacturers may even supply high-quality Al or Cu sheets (or a combination thereof) for testing or local ser-

FIGURE 12 Stack of PMMA slabs on patient support table, used to assess image quality

vice. Phantoms for image quality assessment can also be the same as those used for radiation output measurements (as described in Section 2.3). Depicted in Figure 12 is a set of 35 cm × 43 cm × 2.5 cm PMMA slabs large enough to be imaged with the large FOV image receptors that are used in interventional radiology.

Another type of phantom is multipurpose in design and can be used to test multiple image quality parameters simultaneously. These phantoms often have targets for low-contrast determination, high-contrast assessment, and dynamic range. Some of these phantoms can also be used to assess both positive contrast (simulated iodine or barium) and negative contrast (air). The benefits of these phantoms are that they can be used for multiple tests and often include Cu as an integral part of their makeup, ensuring that the system must respond to a load that is greater than air. Lastly, these phantoms can be used in conjunction with additional patient-equivalent material such as PMMA or Cu to test systems under increased load.

In Figure 13, three well-known multipurpose phantoms are depicted: the IEC 61223-3-1 standard phantom,[31] the Leeds TOR 18FG phantom,[32] and the NEMA XR-21 phantom.[33] All three phantoms are readily available from various vendors.

The NEMA XR-21 phantom was originally developed for II-based imaging chains and was designed for use with analog systems.[33] The central plate of the NEMA XR-21 phantom, which includes iodine-based low-contrast objects and high-contrast line-pair resolution
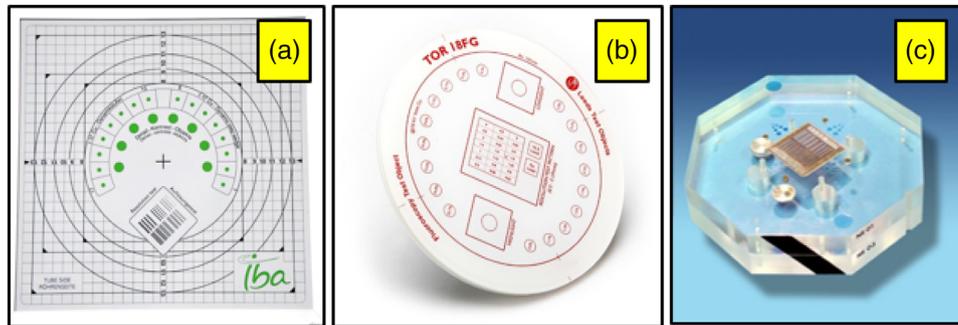
FIGURE 13 Examples of multipurpose phantoms. (a) Photograph of the IEC 61223-3-1 phantom. (b) Photograph of the Leeds TOR-18FG phantom. (c) Photograph of the central plate of the NEMA XR-21 phantom
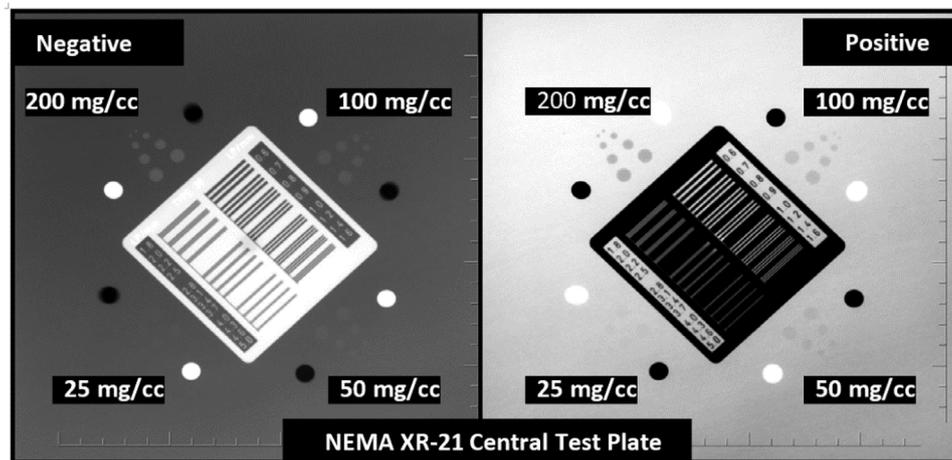
FIGURE 14 Screen-captured images of the NEMA XR-21 phantom central plate both native and inverted. Corresponding iodine concentrations of 200, 100, 50, and 25 mg/cc targets are shown in the images

targets, is nevertheless still a valid QC imaging phantom for digital FPIR systems. Design and fabrication of new image quality phantoms were outside the scope of TG 272; however, the central plate of NEMA XR-21 was consistently used during TG 272 assessments and was used successfully for multiple acceptance tests. Further research is needed to develop a phantom specifically designed to evaluate the CNR-optimized fluoroscopic imaging chain (see Appendix D). For this report, the central plate of NEMA XR-21 was used not as a tool to assess performance but as a tool to test benchmark consistency for future image quality comparisons.

In the middle of the NEMA XR-21, central plate is a line-pair resolution target consisting of lead foil that is 0.1 mm thick (0.6-line pairs/mm to 5.0-line pairs/mm resolution test patterns) (Figure 14). There are four pairs of circular holes (4, 3, 2, and 1 mm in diameter) per set in each of the four quadrants. These holes are filled with iodine concentrations ranging from 25 to 200 mg/cc, with the concentration doubling in each object group.

Depicted in Figure 15 is an artery block phantom[34] developed by Mayo Clinic to enhance the functionality

of the AAPM DSA phantom.[35] This artery block phantom can be used to assess iodine contrast under fluoroscopy or recorded imaging. The phantom includes multiple lesions and aneurysms and multiple sizes to gauge detectability. As is the case with the other phantoms described above, this phantom can be used with additional PMMA to increase the machine output to clinically relevant conditions.

Finally, to assess motion, a rotating wheel or spinning motion phantom can be used to visualize image lag or ghosting. These phantoms can be used for qualitative assessment, the results of which can be used as initial benchmarks during acceptance testing and for later image quality optimization.

2.7.2 | Methods of image quality assessment

Image uniformity
Image uniformity should be evaluated early in acceptance testing to ensure that the FOV and detector are
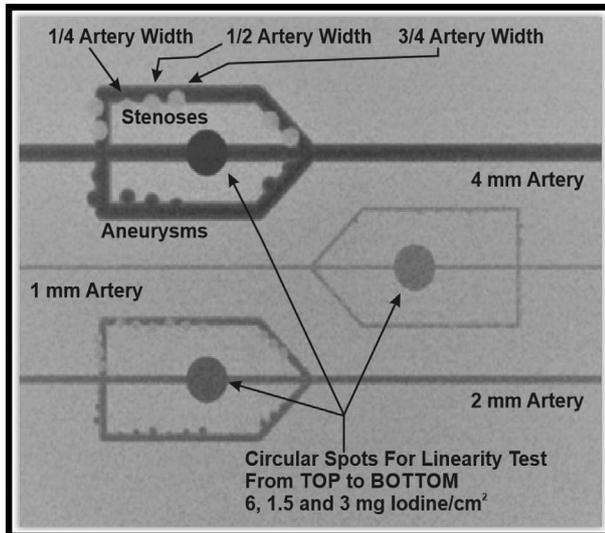
FIGURE 15 A photographically enhanced image of the artery block phantom. Note that the center circular aneurysm areas are excellent spots for region of interest (ROI) placement to determine the CNR for various programs and dose levels. Each blood vessel section is filled with iodine, at concentrations of 6 mg/cm^2 (top), 1.5 mg/cm^2 (middle), or 3 mg/cm^2 (bottom)

TABLE 2 Integral uniformity. Single-shot image using central ROI off grid focus (SID = 95 cm) and at grid focus (SID = 105 cm)

SID (cm)	Maximum pixel value	Minimum pixel value	Integral uniformity
95	2069	1797	7%
105	2080	1876	5%

FIGURE 16 Screen capture of the IEC 61223-3-1–compliant phantom showing the dynamic range available under an examination program and predefined imaging parameters

free from artifacts, dropouts, or nonuniformities created during the installation process. Uniformity can be assessed both qualitatively and quantitatively. A stack of PMMA slabs large enough to be imaged near the detector or Cu sheets (1 or 2 mm) placed on the X-ray tube/collimator port should provide enough load to the system to allow image uniformity to be evaluated. Using ROIs, sections at the periphery can be evaluated by simply comparing the mean pixel values in the periphery to those in the center. If the system does not have the capability to measure pixel values, images can be exported for measurements using DICOM-compatible viewer software. This uniformity test should be performed at several SIDs, including the minimum and maximum SIDs, to ensure that there is no effect from grid cutoff. Most grids used in fluoroscopy utilize a grid ratio with the focal length focused at the midpoint of the SID range. A simple integral uniformity value of a one-frame acquisition may be calculated quantitatively from image pixel data (entire image), as shown in Equation (8):

ducing a small amount of grid cutoff and/or nonuniformity. Results in Table 2 are only for example and are not considered pass/fail, because those values do not exist. This test can be performed on workstations or on most picture archiving and communications systems (PACS).

Dynamic range
Dynamic range can be assessed using one of the multipurpose phantoms shown in Figure 13 or using a step wedge (as shown in Figure 16). Although these tests of dynamic range may not have pass/fail criteria, checking

$$\% \ Integral \ uniformity \ = \frac{(Maximum \ pixel \ value) - (minimum \ pixel \ value)}{(Maximum \ pixel \ value) + (minimum \ pixel \ value)} \times 100. \qquad (8)$$

Table 2 lists sample integral uniformity data obtained at two different SIDs by adjusting the height of the FPIR first to the minimum SID of 95 cm (off grid focus) and then to the SID of 105 cm (at grid focus), thereby intro-

several organ programs may be useful to ensure that the default settings are appropriate. Many of the multipurpose phantoms discussed earlier incorporate a step wedge made of varying thicknesses of Cu as part of

TABLE 3 HCR testing results from fluoroscopy and acquisition modes

Acquisition mode						
FOV size (cm)	48	42	32	22	16	11
Focal spot size (mm)	0.6	0.6	0.6	0.6	0.6	0.6
Pixel size (mm)	0.154	0.154	0.154	0.154	0.154	0.154
Nyquist frequency (1/mm)	3.247	3.247	3.247	3.247	3.247	3.247
Subjective resolution (line pairs/mm)	2.2	2.2	2.2	2.2	2.2	2.2
Fluoroscopy mode						
FOV size (cm)	48	42	32	22	16	11
Focal spot size (mm)	0.6	0.6	0.6	0.6	0.6	0.6
Pixel size (mm)	0.308	0.308	0.154	0.154	0.154	0.154
Nyquist frequency (1/mm)	1.623	1.623	3.247	3.247	3.247	3.247
Subjective resolution (line pairs/mm)	1.4	1.4	2.2	2.2	2.2	2.2

their test patterns. On today's modern systems, visualizing most if not all of the steps on these phantoms should be an easy task. To quantify the dynamic range, the number of unique range steps can be counted (under fluoroscopy mode or acquisition mode). This value is a useful metric to assess each year as long as setup conditions are equivalent.

High-contrast resolution

High-contrast resolution (HCR) can also be evaluated using one of the multipurpose phantoms described above, the central plate described above, or a line-pair resolution phantom, ideally using physics mode. Of all the image quality tests, the HCR test is most sensitive to magnification, focal spot size, and pixel size, factors that are integral to understanding how and why the HCR changes. For this test, note that care should be taken during placement of the phantom to avoid aliasing with the regular pixel matrix.

At minimum, HCR should be assessed for the default calibration FOV to establish a benchmark for periodic QC measurement using the same organ program. The settings used by fluoroscopy and acquisition modes are vastly different (e.g., focal spot, mA, spectral filter); therefore, different results are expected for the different modes. Furthermore, careful attention should be paid to the angle of the bar pattern such that aliasing is minimized on the most visible targets.

Table 3 shows HCR testing results for single-shot acquisition and fluoroscopy modes using the NEMA XR-21 phantom central plate placed in the middle of a 20 cm (8″, inclusive of the XR-21 Phantom) of PMMA under clinical conditions (same imaging system for both modes, abdominal organ program). Placing the phantom in the middle of the PMMA stack more closely approximates clinical conditions in the middle of the body. This arrangement will yield a magnification of roughly 1.5 and, more importantly, is reproducible from year to year. The results in Table 3 are not pass/fail and are shown as

an example of the characterization of the imaging resolution in both fluoroscopy and acquisition modes. Note that the pixel size and focal spot size were determined after assessment using data in the DICOM header. The underlined values show a change in resolution or value observed on the in-room monitor due to a change in the effective pixel size. This is a result of pixel binning, where data from multiple detector elements are combined to improve noise characteristics of the image.

The table shows how the resolution changes with FOV. In acquisition mode, on this unit, there is no apparent increase in resolution, whereas in fluoroscopy, from 42 to 32 cm, there is a change in pixel size (underlined values) that may increase resolution capability.

Low-contrast detectability

Low-contrast detectability is typically used more as an optimization test than as an acceptance test. The variety of phantom types and technical parameters available on the unit being assessed make this test difficult to perform; thus, in the absence of vendor guidance or reference values for a particular phantom, the goal of testing should be to simply establish baseline results for future evaluations. Results of low-contrast detectability are typically reported in a good/better/best format rather than as pass/fail. For acceptance tests of units that primarily use iodine as the contrast agent, the NEMA XR-21 central plate can be used for subjective assessment, and the artery block phantom can be used for both subjective and objective assessment as the targets are large enough for ROI analysis (see Figures 11 and 12).

Image lag, ghosting, and motion

Testing single-image frames from fluoroscopy or single-shot acquisitions is useful when assessing image quality. However, because fluoroscopy uses live images, tests should also be performed on live images. Tests to assess moving image fidelity or the presence of lag (copies of preceding images) need not be complicated and
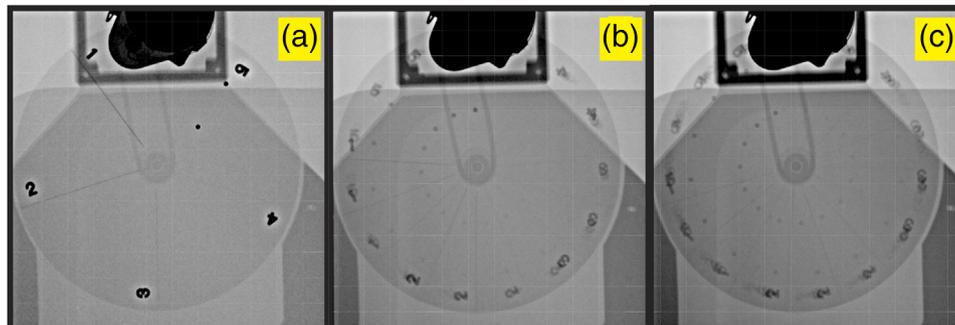
FIGURE 17 Images of the spinning wheel of the NEMA XR-21 phantom. These images were obtained at a fluoroscopic frame rate of 7.5 pps and a pulse width of 3.4 ms. (a) No lag. (b) Some lag. (c) Extreme lag. Note that the images showing some lag (b) and extreme lag (c) demonstrate targets (lead numbers, lead BBs, and varying diameters of piano wires) with more blur or copies of the targets that are smeared because of frame integration over a longer period than the short pulse duration (3.4 ms) of the individual fluoroscopy image (a)

should be reproducible from year to year. Phantoms with motion capability should be used; however, the phantoms should also be imaged while stationary to obtain baseline values (Figure 17). Different results should be expected for static, pulsed fluoroscopy, and recorded imaging data sets.

Tests of motion may also assess the degree of frame averaging in fluoroscopy. Often selectable on the system, frame averaging may be different for different organ/examination programs and may have a dramatic effect on image quality perception in fluoroscopy. Although this motion test is only qualitative, a motion phantom even similar to the NEMA XR-21 phantom may provide useful comparisons of several fluoroscopic settings, which could affect frame averaging and may therefore be a valuable tool for program optimization during fluoroscope setup.

SNR and CNR
In general, SNR and CNR are useful parameters to asses on digital imaging systems to gauge signal, noise, and contrast quantities. However, image processing that is applied internally at the FPIR or downstream from the FPIR makes obtaining these measurements difficult. Obtaining valid raw images for SNR/CNR measurement and analysis requires access beyond that of the basic user level. Furthermore, image processing affects the images presented on the display monitor, and these processed images may not be suitable for acceptance testing or performance evaluation. For these reasons, SNR/CNR measurements are often not included in acceptance testing.

If nonprocessed images are unavailable, a simplistic approach for evaluating SNR/CNR may still be applied to readily available images to establish baseline values. Current SNR optimization ADRC methodology may use a combination of $K_{air,PERP}$, input dose rate to the image receptor, and localized pixel measurements of signal difference-to-noise ratio for different materials to control the system. Although determining $K_{air,PERP}$ and input

dose rate to the image receptor is straightforward, determining CNR (or signal difference-to-noise ratio) is more challenging to illustrate the operation of fluoroscopes. The measurements shown in Figure 18 are from existing QC phantoms or fabricated with readily available materials at the time of testing. Details for saving and analyzing fluoroscopy loops for QC or acceptance testing may be found in Goode et al.[36]

System connectivity
Acceptance tests of imaging systems should also include assessment of basic interoperability. Evaluating image quality during acceptance testing often requires viewing images on PACS or connected workstations to allow for image manipulation and postprocessing. Other downstream systems such as the worklist server or RDIM should also be tested for accuracy. Further tests of interoperability (e.g., alignment of fields from the worklist, parameter display on PACS) and performance/speed should also be performed if any problems in system connectivity are identified. For more information, readers should refer to AAPM Report No. 248, which provides testing methodology.[37]

2.7.3 | Quality control activities

A rigorous QC testing is recommended to ensure that the system is performing consistently over time.[36] A QC program should optimally be set up during acceptance testing before the system is turned over to the end users. The manufacturer's QC program should be followed, as well as any in-house QC programs that are used for similar units. QC often involves performing the motions of imaging before the clinical procedure is initiated to ensure that all of the pieces needed to perform the procedure are in place. Some common mishaps that a simple QC program may detect include spilled contrast on the table, removal and lack of subsequent reinstallation of the antiscatter grid, and dead batteries in the
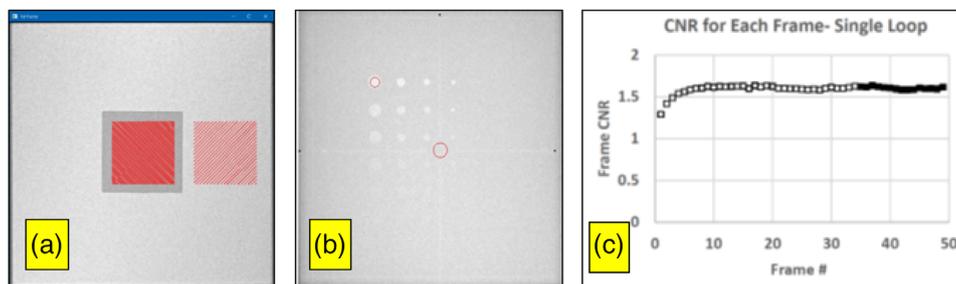
FIGURE 18   The single static images shown in (a) and (b) are frames extracted from a fluoroscopy loop that can be analyzed to determine the CNR under a predefined set of conditions. (a) Uniform background with a contrast target object to mimic Iodine. (b) Custom-fabricated contrast detail phantom. (c) This plot shows the CNR between the two regions for each frame of a fluoroscopy loop obtained from (a), demonstrating the increase in CNR and the steady state that is achieved a few frames later. The blackened squares indicate the frames used to average and calculate a single CNR for the fluoroscopy loop[36]

wireless foot pedal. All of these issues are best discovered before the patient is on the table. A QC program may also detect suboptimal imaging from the unit itself if QC is performed in a reproducible way every day.

For phantoms and devices used to drive the fluoroscope (which range in complexity from a simple Al block or Cu sheet to a phantom containing targets such as a contrast detail scheme), QC testing should focus on reproducibility and objectivity.

QC tests should also focus on the main use of the imaging unit. For example, if the unit is used for fluoroscopy 100% of the time, a single shot-based QC program may not yield information relevant to the clinical use of the unit. At a minimum, tests should collect the parameters for kV, mA, and SSF so that this information may be compared to baseline values established during acceptance testing. More detailed tests of image quality metrics can be performed, but these tests require the use of additional online tools or advanced data collection methods.

3 | MOBILE C-ARM AND INTRAOPERATIVE 2D/3D FLUOROSCOPY SYSTEMS

This section refers to both mobile C-arms and intraoperative 2D/3D fluoroscopy systems. However, in general, when the topics refer to both types of systems, C-arm may be used to mean both systems unless specific to the intraoperative 2D/3D fluoroscopy systems.

3.1 | Mechanical factors

Mobile C-arm fluoroscope gantries are generally manipulated manually, without the precise motor-controlled movements that are used in fixed C-arm fluoroscopes, whereas Intraoperative 2D/3D mechanical movements are moved by motors and X-ray tube-detector motions

are confined to the inner ring. However, all mobile C-arm fluoroscopes have at least a primary and secondary gantry rotation, with either manual or electronic locking mechanisms. These rotations should be inspected to assess ease of movement and the ability of the locking mechanism to hold the gantry in a set position.

To assess mechanical motions for these systems, one rotational locking mechanism should be unlocked at a time to verify that there is smooth and easy gantry movement in each axis of rotation. The gantry should then be relocked, and the lock should be checked to ensure that it holds the gantry in a set position.

The gantries of mobile C-arm fluoroscopes typically include a visual analog indication of the gantry rotation angle, which should also be assessed for accuracy. One exception is C-arm fluoroscopes used for 3D reconstructions, which have automated drive motors with refined angular accuracy. These systems should be evaluated using the process described for stationary fluoroscopes capable of 3D image acquisitions in Section 2.

It should be pointed out that a spacer (cone) is often provided to C-arm fluoroscopy systems to meet with the minimum source-to-skin distance (SSD) requirement. It is suggested to ensure that the spacer is indeed available and provide the minimum required SSD.

3.2 | X-ray generator and radiological parameter accuracy

The generator of a mobile C-arm unit mirrors that of a stationary C-arm unit; therefore, the tests for these units will largely be the same, with a few exceptions. For ease of testing, mobile C-arms can generally be unlocked and geometrically inverted from the typical clinical orientation, resulting in the X-ray tube being situated at the top of the C-arm with the image receptor at the bottom. Regardless of image receptor type, care must be taken to protect the image receptor from burn-in artifacts during measurements. This is usually accomplished by

using lead sheets or multiple layers of protective garments.

Generator testing of mobile fluoroscopes can often be performed in either a fluoroscopic or radiographic mode (when available). Although either operating mode can be used, radiographic mode is generally preferable because of the higher tube output rates associated with this technique. Tube outputs at lower kV stations (<60 kV) may be too low to trigger noninvasive measurement devices, possibly necessitating a reduction in the focal spot-to-device distance to obtain a measurement.

Although nearly all mobile C-arms allow manual control of the tube potential (kV), tube current (mA) is often automatically indexed to the kV setting and not individually adjustable, making linearity measurements difficult. However, some models of C-arm systems do allow for independent control of both tube potential and tube current. For C-arms without individually adjustable mA settings, single-shot radiographic acquisitions sometimes use an automatic exposure control feature that makes use of a fixed kV and adjusts the mAs according to attenuation in the beam path. For these types of units, exposure linearity can be measured by adding increasing amounts of attenuating material to the beam path.

Finally, if there are multiple buttons or pedals that can initiate the X-ray beam, all buttons and pedals should be tested for proper functionality.

3.2.1 | Peak tube potential (kV)

The kV for mobile fluoroscopes should be evaluated at a minimum of three stations covering the span of clinically achievable values, generally from 50 to 60 kV through 110 to 120 kV. Measurements can be made in both fluoroscopy and acquisition (radiographic) mode if desired, although both modes should yield similar measurements. Displayed kV should correspond to measured values within manufacturer specifications or within ±10% of the indicated kV. For more details regarding fluoroscopy mode, see Appendix A, Fluoroscopy Tube Potential Accuracy; for more details regarding acquisition mode, see Appendix A, Acquisition Mode.

3.2.2 | Tube current/mAs linearity

For mobile fluoroscopes that allow manual kV adjustment, the mAs should be evaluated at a minimum of three mAs stations covering the span of clinically achievable values. Calculated mGy/mAs values at the various mAs stations should all be within ±10% of each other.

For mobile fluoroscopes that do not have manually adjustable mAs but use an ADRC system to determine mAs for single-shot radiographic acquisitions, the tube current/mAs linearity should be assessed as follows:

- Place a minimal amount of an attenuating medium (e.g., 2–5 cm of PMMA) on the image receptor.
- Orient the measuring device free-in-air around the primary beam axis of the C-arm gantry.
- Take a radiographic exposure.
- Increase the PMMA thickness and repeat the previous steps, ensuring that the kV is constant. Tube voltage is likely to remain constant for acquisitions as long as fluoroscopy is not engaged.
- Plot the mGy/mAs and ensure linearity to within ±10%.

3.2.3 | HVL

Verify that the minimum regulatory required HVL is met using methods prescribed in Section 2.2.2.

3.3 | Radiation output measurements

3.3.1 | Radiation output as a function of PMMA thickness

During acceptance testing, radiation output and variations in technique parameters such as kV, mA, and/or pulse width can be measured as a function of increasing PMMA thickness in various fluoroscopy protocols to determine the operating characteristics of the mobile imaging system. This information allows examination protocols and operating modes to be matched to specific clinical tasks and provides baseline data for future troubleshooting.

The vendor or the user manual should be consulted to determine whether different examination protocols are driven by unique fluoroscopy curves or if they only indicate changes in image processing, as this information may not be obvious to the user. On systems with a large number of available protocols, this test of radiation output need only be performed for protocols with unique fluoroscopy curves, as changes in image processing will not change the acquisition parameters.

This test should be performed using the procedure described in Section 2.3.2. For ongoing annual testing beyond acceptance, the entire test does not need to be repeated; typical patient entrance exposure rates can be measured for selected protocols, frame rates, and/or magnifications to verify constant performance over time and to compare mobile C-arm systems.

3.3.2 | Maximum AKR

In fluoroscopic imaging mode, the maximum AKR is defined for all mobile C-arms with a maximum SID greater than 45 cm at a plane 30 cm from the input of the fluoroscopic imaging assembly.[5,6] The maximum AKR

should be tested free-in-air with narrow-beam geometry (using a well-collimated field) either in or corrected to the designated plane. The maximum AKR allowable by the FDA is 88 mGy/min in normal mode of operation and 176 mGy/min in high-level or boost operating mode. During testing, the continuous audible signal that is required to sound when air kerma limits exceed 88 mGy/min in high-level operating mode should be assessed for proper function.

As with all fluoroscopic systems, there are no AKR limitations in the acquisition or radiographic modes of operation, although mobile C-arms generally limited in their acquisition capabilities.

3.3.3 | Dose and dose rate at the PERP

Follow the procedure described in Section 2.3.3.

3.3.4 | Image receptor input dose and dose rate

On most mobile C-arm systems, the grid is fixed to the detector behind the cover and cannot be accessed without some level of disassembly. For this reason, measurement of the detector input dose and dose rate is not generally recommended.

3.3.5 | Displayed PERP dose verification

Unless otherwise stated by the manufacturer, the TG 190 PERP for all full-size mobile C-arm systems is 30 cm from the image receptor assembly entrance surface, the same location specified by the FDA for determination of the maximum allowable dose rate limit.[5]

> **NOTE 9**: For all but interventional C-arms, there is no IEC definition for the RP (the PERP). However, vendors report the location of the PERP in their accompanying documentation. Often, C-arm manufacturers follow FDA regulations for defining the PERP (hence, 30 cm from the image receptor).

3.4 | Collimator congruence test

Collimator congruence tests should be conducted similar fashion as in Section 2.4.

3.5 | Display monitors

Evaluation of display monitors for mobile C-arm fluoroscopes should be performed using the procedures outlined in Section 2.5, although adjustability of luminance levels for mobile monitors and the ability to load outside test patterns may be more limited on these mobile systems. All available monitors should be evaluated under expected operational ambient light conditions. L_{min} and L_{max} should be measured, LR should be calculated, and both quantitative (LUDM) and qualitative uniformity assessments should be performed.

3.6 | Fluoroscopic dose monitoring and tracking

Dose monitoring and tracking are required for mobile C-arm fluoroscopy systems. Attenuation factors of clinically used examination tables and mattresses can be measured using the methods described in Section 2.6; however, a given C-arm unit may use a variety of examination table/mattress combinations such that only a general or average table/mattress factor can be determined.

3.7 | Image quality assessment

Image quality for mobile systems should be assessed as outlined in Section 2.7, using similar phantoms. At a minimum, HCR and low-contrast detectability should be evaluated, as required by Joint Commission standards.

3.8 | Specific tests for intraoperative 2D/3D fluoroscopy

There is a limited number of intraoperative 2D/3D fluoroscopy systems on the commercial market. They include: (1) Medtronic intraoperative 2D/3D system, otherwise known as O-arm, (2) Ziehm Vision RFD 3D, (3) GE-OEC 3D, and (4) Siemens Cios Spin. Systems (2)–(4) are extension of C-arm fluoroscopy capability. The O-arm is designed to perform both 2D fluoroscopy and 3D imaging for image-guided operations such as spine fusions and is not a C-arm based system. Typically, 2D fluoroscopy is used to position the system in preparation for 3D imaging, and 3D imaging is used to reconstruct images from pulsed X-ray exposures that are obtained during a complete 360° rotation of the tube within the gantry around the patient. The 3D acquisition can be obtained with either standard mode or high-resolution mode, which uses twice the number of projections as standard mode. All 3D acquisitions are obtained using programmed techniques that do not automatically modulate during the scan.

For acceptance testing, benchmark measurements should be obtained in both 2D and 3D modes of operation to ensure proper functioning. Note that an intraoperative 2D/3D is classified by the FDA as a

mobile fluoroscopy unit; thus, as of the time of this publication, only fluoroscopy FDA regulations apply to this type of system (barring any state-specific regulations).

3.8.1 | 2D fluoroscopy

Tests for 2D fluoroscopy can be performed following the protocols described previously in Section 2.3. Note that the tube and detector assembly on these systems can be rotated such that the tube is overhead, allowing for easier setup of phantoms and meters.

Despite its use primarily as a 3D imaging device, the Medtronic O-arm is classified by the FDA as a mobile fluoroscopy unit. Consequently, it must adhere to maximum tube output regulations in 2D imaging mode. The maximum output for 2D imaging mode must be measured 30 cm from the outer plastic cover placed over the image receptor (83 cm from the focal spot). This is not the same location as the PERP for the displayed air kerma, which the vendor reports to be 15 cm toward the X-ray tube from isocenter, or 50 cm from the focal spot.

The on-screen displayed air kerma often exceeds the FDA maximum air kerma limits in 2D fluoroscopy mode; thus, Medtronic does not recommend extended 2D imaging with the patient at isocenter.

3.8.2 | 3D acquisition

For rotational angiography equipment, a method suggested by Medtronic is to use the computed tomography dose index (CTDI) body phantom to measure dosimetry and the ACR CT phantom to measure image quality.

Briefly, because of the wide cone-beam projections in the Intraoperative 2D/3D, the concept of CTDI for dose profiles up to 100 mm is not valid for these systems. The correct way to measure the dose on these units is to position a small volume chamber at the center and at the periphery of a phantom that is long enough to accommodate all scatter to the longitudinal center. The manufacturer, however, still uses the 100-mm CTDI chamber to report $CTDI_{vol}$ on standard CT dose phantoms (16- and 32-cm CTDI phantoms), which underestimates the dose. In practice, dose phantom selection depends on the anatomy protocol. For example, the 16-cm phantom is used for head and neck protocols, and the 32-cm phantom is used for chest, abdomen, pelvis, and leg protocols. The 100-mm chamber can be used to test the difference between the measured and displayed $CTDI_{vol}$; a difference of $\leq 20\%$ between these values is recommended. Note that the system uses 120 kV for all 3D imaging but scales mAs values based on patient size. Therefore, dosimetry testing can be performed for one patient size, and other CTDI values for various patient sizes (small, medium, large, and extra large) can then be linearly scaled. Other methods for evaluating constancy
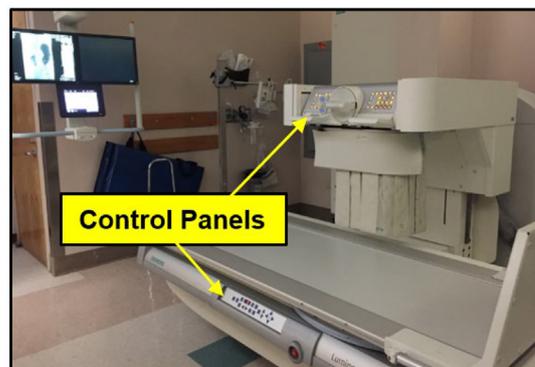
FIGURE 19 Conventional fluoroscopy system. An FPIR system is shown here. The X-ray tube is installed under the tabletop and enclosed in the table side panels

using smaller chambers in air are also acceptable; however, there is no reference for these values in manufacturer documentation.

Because the 3D acquisition of this system is designed mainly to visualize and measure high-contrast objects, the high-contrast module of the ACR CT phantom can be used to assess spatial resolution. A resolution ≥ 6 line pairs/cm is recommended.

4 | CONVENTIONAL FLUOROSCOPY

A conventional fluoroscopy system is built around a floating patient table, which can be rotated to a vertical position. The fluoroscopy X-ray tube is installed under the patient table, and the II or digital FPIR is installed above the table (Figure 19).

4.1 | Mechanical factors

The mechanical integrity and smooth operation of the examination tabletop and the fluoroscopy table/pedestal assembly should be evaluated during acceptance testing. These tests should be conducted not only at the tableside control panel (Figure 20), but also at the control panel located at the FPIR tower assembly (see Figure 19). These two control panels are similar to each other in function, but the specifics of which functionalities are available at each location vary by vendor.

The following factors should be assessed:

- Tabletop motion: The floating table can be moved left, right, forward, and backward.
- Table angulation: The floating table can smoothly rotate up to 90°, in both counterclockwise (−) and clockwise (+) directions, although some systems have a limited angulation of −30° (Trendelenburg or head down position).
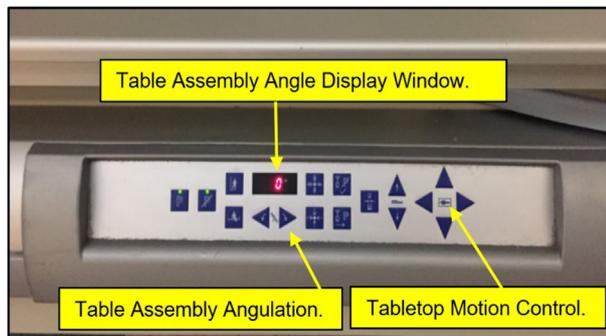
FIGURE 20 The tableside control panel for the examination table. Adjustments to control tabletop motion, table assembly angulation, and angle display window are available

FIGURE 22 The experimental setup for measuring radiation output on a conventional fluoroscopy system. Note X-ray tube under table with a fixed SSD

FIGURE 21 Fluoroscopy suite with overhead radiographic X-ray tube

- Alignment and centering with the overhead radiographic tube: In most conventional fluoroscopy rooms, there is an overhead radiographic tube that can be used in conjunction with the fluoroscopy table to function as a radiographic system (Figure 21). Alignment and centering between the fluoroscopy table and the radiographic tube should be assessed.
- Radiation shielding apparatus: The shielding apparatus should be assessed to identify any possible damage. The installation of the shielding apparatus should also be checked to ensure proper shielding of operators at typical positions.

4.2 | X-ray generator and radiological parameter accuracy

Generator parameter accuracy measurements (including X-ray tube potential, tube current, mAs linearity, and HVL) should be assessed as outlined in Section 2.

4.3 | Radiation output measurements

4.3.1 | Radiation output as a function of PMMA thickness

The experimental setup for measuring radiation output is shown in Figure 22. The detailed procedures are also described below.

4.3.2 | Maximum AKR

For conventional fluoroscopy systems in which the X-ray tube is installed under the examination table, the maximum fluoroscopic AKR limitations for all available FOVs should be tested under normal and boost modes with the radiation detector placed 1 cm above the tabletop in accordance with FDA regulations. Typically, the image receptor tower assembly is raised at least 30 cm from the tabletop to simulate clinical conditions. However, the maximum SID (~100 cm) may be employed to ensure consistency in measurements from year to year.

For regulatory maximum AKR measurements, in-air geometry with no scatter material in the primary beam (with the exception of the examination tabletop) should be used.

4.3.3 | Dose and dose rate at PERP

Follow the procedure described in Section 2.3.3, with the PERP placed 1 cm above the tabletop without a mattress.

4.3.4 | Image receptor input dose and dose rate

If the grid can be removed, a geometrical correction can be applied to the FPIR measurement to calculate the dose rate at the level of the detector surface. For cases in which the grid is not removable, vendors can sometimes supply a grid correction factor that can be applied to input surface measurements to account for attenuation of the grid and to allow for calculation of detector input dose rates. As mentioned in Section 2.3.4, image receptor input dose rates can be useful for measuring baseline performance but are not absolutely necessary for acceptance testing.

4.3.5 | Displayed PERP dose verification

Follow the procedure described in Section 2.3.5.

4.4 | Collimator congruence test

Follow the procedure described in Sections 2.4.1 and 2.4.2 for the posteroanterior direction with the table angulation set at $\pm 30°, 45°$, and $90°$.

4.5 | Display monitors

Follow the procedure described in Section 2.5.

4.6 | Fluoroscopic dose monitoring and tracking

4.6.1 | TG 190 dose correction

All available displayed radiation doses (reference air kerma, dose-area product, KAP) should be verified per the protocols described in AAPM Report No. 190.[9] The PERP for cumulative air kerma on systems in which the X-ray tube is installed under the examination table is typically the same as the FDA-specified maximum dose point: 1 cm above the tabletop. Hence, the mattress should not include.

4.6.2 | Patient comfort mattress attenuation correction

Because the X-ray tube assembly is under the table, the patient's skin is exposed at all times with transmission through the mattress and tabletop. However, depending on how the $K_{air,PERP}$ and air KAP are defined, the verification of the PERP needs to be confirmed to conform with the specific manufacturer setup.

4.7 | Image quality assessment

Image quality should be assessed as outlined in Section 2.7, using similar phantoms. At a minimum, HCR and low-contrast detectability should be evaluated, as required by Joint Commission standards.

5 | OVERHEAD-TYPE FLUOROSCOPY

Overhead-type fluoroscopy (OHTF) systems present several challenges for acceptance testing. First, as the name implies, OHTF systems are inverted with respect to the X-ray tube and image receptor configuration, presenting a geometry that is unfavorable to the operating staff from a radiation safety perspective. In systems with the X-ray tube assembly installed under the examination table, the scatter profile in the room is typically directed toward the floor. With OHTF geometry, the scatter profile is directed toward the torso and head of the operator. Therefore, acceptance testing for OHTF systems should include scrutiny of available radiation shielding devices such as moveable shields and leaded glasses[38] so that staff can avoid lens injury.[39]

Second, OHTF systems typically have both radiographic and fluoroscopic capabilities, which complicate acceptance testing. The procedures performed using OHTF units (e.g., video urodynamics and cystoscopy) require scanning through the pelvis (often while the patient is sitting) and imaging bone, fat, air, and contrast, necessitating a high dynamic range. These systems may also include a micturition chair that is attached to the table, with the gantry rotated upward at $90°$.

In addition, OHTF systems are often equipped with control panels attached to the examination table and on a mobile pedestal, the functionalities and proper operation of these controllers should also be verified.

NOTE 9: OHTF systems designed for upper/lower GI examinations fall within this category of fluoroscopy imaging systems, although these systems are often referred to as "remote-controlled" fluoroscopy systems, as radiologists work in the control booth behind protective shielding. Some room configurations therefore present opportunities for the radiologist/operator to be remoted and not receive scatter from patients being imaged on the OHTF system.
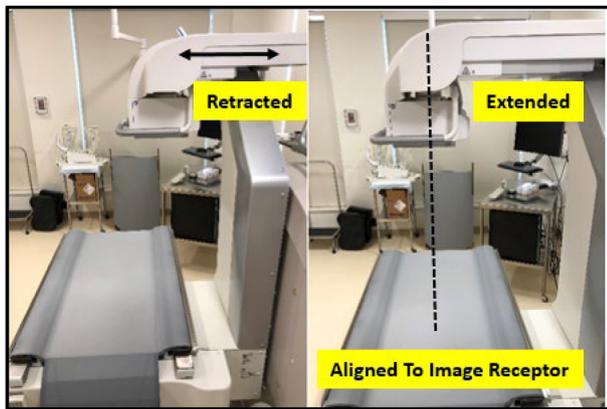
FIGURE 23 The "park" location of the X-ray tube (retracted, on the left) and the "operation" location of the X-ray tube (extended, on the right) on an OHTF system

5.1 | Mechanical factors

5.1.1 | Tabletop motion

OHTF systems typically have relatively short tabletops (compared to those used in typical fluoroscopy systems) with multiple add-ons to the table that allow for various imaging setups. The table and add-ons should be tested for ease of motion and secure attachment, and the room should be checked for pinch points during mechanical motions when add-ons are installed.

5.1.2 | Verification of SID

OHTF systems designed for upper/lower gastrointestinal examinations are often equipped with variable SID. The SID selection and the accuracy of SID should therefore be verified during acceptance testing.

5.1.3 | Alignment and centering with overhead fluoroscopic tube

Because of the variety of configuration options available on OHTF systems, the tube head may have several degrees of freedom, including the ability to move out of the way to allow a patient to be loaded onto the table. These degrees of freedom provide opportunities for misalignment between the tube and receptor and should therefore be assessed during acceptance testing. Furthermore, a safety switch check should be performed to ensure that no X-rays can be generated if the X-ray tube assembly is not interlocked over the image receptor. Many of these systems (e.g., urology and cystoscopy) incorporate a fixed SID. Figure 23 shows two of these possible tube motions/positions.

As shown in Figure 24, many systems also have the ability to couple the X-ray tube with the image receptor

and move them as one assembly. The images in Figure 24 show translation of the X-ray tube and the image receptor motion; these motions should be assessed to ensure proper alignment once the assembly is locked.

The centering of the X-ray central beam with the image receptor should also be evaluated to ensure radiation beam alignment. Because the image receptor is installed just under the tabletop, the procedure described in Section 2.4.2 must be modified to account for configuration differences.

5.2 | X-ray generator and radiological parameter accuracy

Generator parameter accuracy should be measured following the procedure described in Section 2.2. The presence of radiographic and fluoroscopic functionality should ease testing.

5.3 | Radiation output measurements

5.3.1 | Radiation output as a function of PMMA thickness

Figure 22 shows the proper setup to measure patient dose rates. Note the inverted geometry and the need for fixation of ionization chamber or SSDS.

5.3.2 | Maximum AKR

The maximum radiation output (dose and dose rate) on OHTF systems must be measured using in-air geometry in the absence of any scattering material. The output must be calibrated so that it does not exceed the regulatory allowable limits set for corresponding operational modes. Specifically, the maximum AKR must not exceed 88 mGy/min in regular mode and 176 mGy/min in high-level control or boost mode. The FDA has stated that a measurement point 30 cm from the tabletop should be used to determine the maximum allowable output.[40]

5.3.3 | Dose and dose rate at the PERP

Patient entrance dose should be measured following the procedure used for other systems; however, for OHTF, the system is inverted. Figure 25 shows an SSDS in the beam with PMMA stacked on the table. Regardless of PMMA thickness, corrections must be made to 30 cm from the tabletop.

If an SSDS is used, selecting particular fields to measure (for fluoroscopy) away from the SSDS may avoid driving up the ADRC. These fields can also be tested by covering corresponding areas with Cu or Al and

FIGURE 24 Left: Longitudinal translation of the tube assembly is not aligned to the image receptor. Right: The alignment is centered with the image receptor, and the assembly is locked for imaging in fluoroscopy mode or radiography/acquisition mode, as required
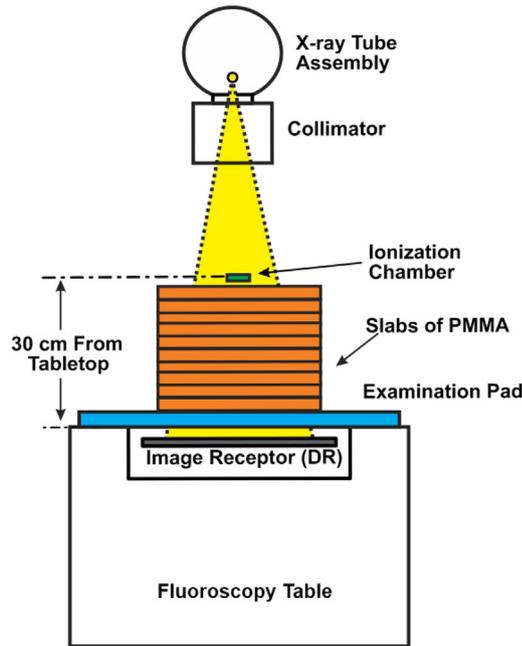
FIGURE 25 Experimental setup for measuring radiation output. Care must be taken to avoid driving the ADRC with SSDS. An ionization chamber works well in these situations and can be left in the same position for testing all slab thicknesses. Doses can then be corrected for 30 cm from the tabletop

FIGURE 26 Software control panel showing nine selections of sensing areas for the ADRC of the image receptor for fluoroscopy. In each of these nine selections, a black rectangular box represents an active sensing area. Note that control sensing areas can be programmed for multiple or single locations by selecting one of these nine setups. The setup shown in the lower right corner represents a situation in which the entire image receptor is active as the ADRC sensor

determining whether the area selected is still being used as a dominant sensor for the ADRC (as shown in Figure 26).

5.3.4 | Image receptor input dose and dose rate

In OHTF systems, the receptor is located under the table. Unless the vendor provides access to the area under the table, the flat panel dose can be measured only on top of the table.

5.3.5 | Displayed PERP dose verification

Consult the vendor's technical manual for information about PERP. Typically, the PERP is 30 cm above the tabletop.

5.4 | Collimator congruence test

On many of these systems, a two-step verification process may be necessary to assess the congruence between light and radiation field and between radiation field and displayed image. Refer to Section 2.4 for further information.

5.4.1 | Light field illuminance test

If a light field for radiographic imaging is in place, the light field illuminance should be assessed to ensure that it meets regulations. Refer to state regulations for light illuminance minimum requirements.

5.4.2 | Light to radiation field congruence

This test can be performed using a computed radiography plate, Gafchromic film, or other independent external media. Rulers or other markers should be used to compare the exposed area on the media with the light field for the head, the foot, and the left and right directions.

5.4.3 | Radiation field to displayed image congruence

Once congruence between light and radiation field has been established, congruence between the radiation field and the displayed image on the monitor should be assessed. This test not only verifies the visual accuracy of the displayed image but also ensures that the radiation does not fall outside of the fluoroscopic image receptor and that it tracks appropriately for all magnification modes. Refer to Section 2.4.

5.5 | Display monitors

Display monitors should be tested using the procedure described in Section 2.5.

5.6 | Fluoroscopic dose monitoring and tracking

5.6.1 | TG 190 dose correction

Refer to Section 2.6.1 for accuracy of KAP meters.

5.6.2 | Examination mattress attenuation correction

Because the tube-receptor configuration is inverted on these units, the skin is exposed without transmission through the mattress or tabletop; therefore, no corrections for tabletop or mattress are required for skin dose calculations.

5.7 | Image quality assessment

Dynamic range is a crucial part of image quality assessment for OHTF systems. The patients imaged on these systems can be quite large. Additionally, systems used for urology often do not have high kW ratings, making high dose rate fluoroscopy (>88 mGy/min) unachievable. In many cases, because of these factors, fluoroscopic image quality may be insufficient, and in extreme cases, acquisitions may be used to obtain needed imaging details. Thus, adequate assessment of both fluoroscopy and recorded image quality may be necessary. Consult the image quality Section 2.7 of this report for more information regarding the multipurpose image quality phantoms that should be used for these tests.

6 | MINI C-ARM FLUOROSCOPY

Mini C-arm fluoroscopy systems are C-arm systems with a maximum SID < 45 cm that are used to image the extremities. The SSD of these systems should be >19 cm for general extremity use but could be as low as 10 cm for specific surgical applications that require a shorter SSD.[40]

6.1 | Mechanical factors

The following parameters should be verified at the time of acceptance testing for mini C-arm systems:

- The SID should be <45 cm.
- The SSD should be >19 cm for systems used for general extremity imaging.
- The SSD should be ≥10 cm for systems used for specific surgical applications.
- A label stating "For extremity use only" should be affixed to mini C-arm systems used for general extremity imaging.
- The accuracy of the laser alignment should be assessed.
- A visible mark should be placed for focus location.
- The mechanical stability of the mini C-arm gantry should be evaluated.
- All pivots and locks should be assessed to ensure smooth motion.

6.2 | X-ray generator and radiological parameter accuracy

Most mini C-arm fluoroscopy systems allow for manual control of tube potential, which enables relatively straightforward measurement of X-ray generator parameter accuracy.

6.2.1 | Tube potential (kV)

Tube potential should be measured as follows:

- Place an appropriate attenuation material (>1/32-inch lead or 2-mm Cu sheet) on top of the image receptor assembly to protect the image receptor from multiple exposures for kV measurements.

- Position the noninvasive kV meter (or SSDS radiation probe) 10–20 cm from the surface of the image receptor housing assembly.
- Measure the tube potential under fluoroscopy using manual kV adjustment if available.
- Ensure that the measured kV is within the manufacturer's specification or within a tolerance of $\pm 10\%$.
- Repeat the last two steps for radiographic mode.

6.2.2 | Tube current (μA) or tube current–time product (μAs)

Most mini C-arm systems do not allow for manual adjustment of tube current decoupled from changes in the kV setting, so independent tube current and linearity cannot be measured.

6.2.3 | Exposure time

Most mini C-arm systems do not allow for adjustment of pulse width or exposure time; however, pulse width (ms) can be measured and displayed pulse rate (pps) can be verified with most modern SSDS. Follow the procedure described in Section 2.2.3.

6.2.4 | HVL (mm Al)

Follow the procedure described in Section 2.2.5.

6.2.5 | Total filtration (mm Al)

Follow the procedure described in Section 2.2.6.

6.3 | Radiation output measurements

As mentioned previously, the practical measurement of technique parameters can be performed at any point on the central axis. However, 21CFR1020.32(d)(3)(iv) states that for mini C-arm fluoroscopes with an SID < 45 cm, the maximum AKR should be measured at the minimum SSD.[5]

6.3.1 | Radiation output as a function of PMMA thickness

On mini C-arm systems, radiation output and technique parameters such as kV, μA, and/or pulse width can be measured as a function of PMMA thickness in various clinical modes of operation including fluoroscopy, snapshot, and cine modes. To simulate typical extremity sizes, the PMMA thickness can be varied from 2 to 15 cm in 1-cm increments.

6.3.2 | Maximum AKR

Because mini C-arm systems are designed for extremity use only, the maximum output with maximum kV is easily reached with a PMMA thickness of 15 cm or a 1/32-inch lead sheet. The PERP employed for the displayed dose and dose rate for mini C-arms is not defined uniformly across various vendors.

6.3.3 | Dose and dose rate at the PERP

Follow the procedure described in Section 2.3.3.

6.3.4 | Image receptor input dose and dose rate

For most mobile C-arm systems inclusive of mini C-arm fluoroscopy, the grid is fixed in place behind the protective cover of the image receptor assembly. Therefore, the grid cannot be accessed without some level of disassembly. For this reason, measurement of the image receptor input dose and dose rate is not generally recommended.

6.3.5 | Displayed PERP dose verification

The first step in evaluating the accuracy of AKR on mini C-arm systems is to obtain the PERP from the operator's manual, as federal regulations do not specify a standard location for the PERP. Typical RP locations are 2 or 5 cm from the image receptor assembly; thus, distance corrections may be needed to adjust the value from a measured AKR to a displayed AKR. TG 272 strongly recommends that the PERP for the displayed AKR for mini C-arm equipment should be uniformly defined as 10 cm from the image receptor assembly.

6.4 | Collimator congruence test

Follow the procedure outlined in Section 2.4 for all available FOVs. Typical mini C-arm systems may not be equipped with a manual collimating feature but may have two different FOVs.

6.5 | Display monitors

Display monitor testing should be performed following the procedure described in Section 2.5. Mini C-arm systems are typically used in brightly lit emergency departments, surgical suites, and cast rooms. For this reason, special attention is required when attempting to match the ambient lighting conditions used in testing to the lighting conditions used clinically.

6.6 | Fluoroscopic dose monitoring and tracking: TG 190 dose correction

The area for the displayed KAP for mini C-arm systems does not actively change but can be calculated based on the size of the default FOVs from the image receptor. However, the PERP of mini C-arm systems varies from one manufacturer to another and often from one version of software to another for the same unit. If patient dose monitoring is desired, the location of the PERP must therefore be verified, and the displayed PSD must be normalized/standardized if multiple models and/or brands of mini C-arm systems are used within an institution.

6.7 | Image quality assessment

Follow the procedure described in Section 2.7. At a minimum, HCR and low-contrast detectability should be evaluated, as required by Joint Commission standards. Note that because of the small FOV, sections of the test tools may need to be imaged separately for different image quality metrics. Additionally, any added attenuator used in conjunction with a test tool should be clinically relevant (e.g., 5 cm of PMMA phantom).

7 | DISCUSSION

The main focus of this report is acceptance testing; thus, no attempt has been made to recommend which parameters need to be evaluated on a periodic basis or how often these tests should be performed. Annual equipment testing, for instance, may be a subset of acceptance testing. However, the frequency of testing required for the various physical parameters can differ substantially. For instance, parameters such as tube potential and HVL, which are not likely to change substantially over a 1-year period, may be categorized as requiring only annual evaluation. On an annual basis, a reduced number of physical parameters may be evaluated in addition to the parameters that must be assessed to meet regulations, such as the alignment and congruence of the radiation field and the image receptor. Two Institute of Physics and Engineering in Medicine Topical Reports discuss the parameters to be evaluated and the suggested frequency of assessments in further detail.[41,42]

The total time required to perform the acceptance tests described in this document will vary substantially depending on the modality. For the most intensive testing procedures on the most complex units (e.g., cardiovascular and visceral interventional units), the physicist should plan for 12–16 h of testing per imaging plane. Other types of units should require less time, depending on the physicist's familiarity with the control functions. Ideally, irrespective of the modality, time should be included in the installation schedule for acceptance testing to be performed by the medical physicist.

DISCLOSURE STATEMENT

The members of AAPM TG 272 attest that they have no potential Conflicts of Interest related to the subject matter or materials presented in this document. The Chair of the AAPM TG 272 has reviewed the required Conflict of Interest statement on file for each member of AAPM TG 272 and determined that disclosure of potential conflicts of interest is an adequate management plan. Disclosures of potential conflicts of interest for each member of AAPM TG 272 are found at the close of this document. In addition, there is no funding sources provided to this task group or any of the task group members in relation to this report.

REFERENCES

1. National Electrical Manufacturers Association. *NEMA XR 27–2013 (R2018): X-ray Equipment for Interventional Procedures User Quality Control Mode*. National Electrical Manufacturers Association; 2019.
2. International Electrotechnical Commission. *IEC 60601-2-43:2010+AMD1:2017+AMD2:2019 CSV, Consolidated Version*. Medical electrical equipment – Part 2–43: particular requirements for the basic safety and essential performance of X-ray equipment for interventional procedures. International Electrotechnical Commission; 2019.
3. Digital Imaging and Communications in Medicine. *PS 3.3-2003: Part 3: Information Object Definitions*. C.8.7.4.1: X-ray table attribute description. National Electrical Manufacturers Association; 2003.
4. US Food and Drug Administration. *Code of Federal Regulations Title 21. Performance Standards for Ionizing Radiation Emitting Products, Section 1020.30: Diagnostic x-ray systems and their major components. (m) Beam quality (1) Half-value layer (HVL)*. Food and Drug Administration; 2019.
5. US Food and Drug Administration. *Code of Federal Regulations Title 21. Performance Standards for Ionizing Radiation Emitting Products, Section 1020.32: Fluoroscopy Equipment. (d) Air Kerma Rates*. US Food and Drug Administration; 2019.
6. Suggested State Regulations for Control of Radiation, Part F, Section F.5 (e)(iv)(3). Conference of Radiation Control Program Directors, Inc. 112 East Main Street, Suite 1, Frankfort, KY 40601
7. Lin PJ, Rauch P, Balter S, et al. *AAPM Report No. 125: Functionality and Operation of Fluoroscopic Automatic Brightness Control/Automatic Dose Rate Control Logic in Modern Cardiovascular and Interventional Angiography Systems*. American Association of Physicists in Medicine; 2012.
8. Rauch P, Lin PJ, Balter S, et al. Functionality and operation of fluoroscopic automatic brightness control/automatic dose rate control logic in modern cardiovascular and interventional angiography systems: a report of Task Group 125 Radiography/Fluoroscopy Subcommittee, Imaging Physics Committee, Science Council. *Med Phys*. 2012;39:2826-2828.
9. Lin PJ. The operation logic of automatic dose control of fluoroscopy system in conjunction with spectral shaping filters. *Med Phys*. 2007;34(8):3169-3172.
10. Lin PJ, Schueler BA, Balter S, et al. Accuracy and calibration of integrated radiation output indicators in diagnostic radiology: a report of the AAPM Imaging Physics Committee Task Group 190. *Med Phys*. 2015;42:6815-6829.
11. Shepard SJ, Lin PJ, Boone JM, et al. *AAPM Report No. 74: Quality Control in Diagnostic Radiology: Report of Task Group #12 of*

Diagnostic X-Ray Imaging Committee. American Association of Physicists in Medicine; 2002.

12. US Food and Drug Administration. Resource Manual for Compliance Test Parameters of Diagnostic X-Ray Systems. Field Limitation and Alignment. https://www.fda.gov/Radiation-EmittingProducts/RadiationEmittingProductsandProcedures/MedicalImaging/MedicalX-Rays/ucm115361.htm#III. Accessed November 3, 2020.

13. Lin PJ. A device for checking alignment of fluoroscopic systems. *Opt Eng*. 1977;16:163302.

14. Bevins NB, Flynn MJ, Silosky MS, et al. *AAPM Report No. 270: Display Quality Assurance*. American Association of Physicists in Medicine; 2019.

15. Bevins NB, Silosky MS, Badano A, Marsh RM, Flynn MJ, Walz-Flannigan AI. Practical application of AAPM Report 270 in display quality assurance: a report of Task Group 270. *Med Phys*. 2020;47:e920-e928.

16. ACR–AAPM–SIIM Technical Standard for Electronic Practice of Medical Imaging. Revised 2017 (Resolution 41). https://www.acr.org/-/media/ACR/Files/Practice-Parameters/Elec-Practice-MedImag.pdf. Accessed November 3, 2020.

17. Silosky MS, Marsh RM. Performance characteristics and quality assurance considerations for displays used in interventional radiology and cardiac catheterization facilities. *J Appl Clin Med Phys*. 2018;19:708-717.

18. Samei E, Badano AI, Chakraborty D, et al. Assessment of display performance for medical imaging systems: executive summary of AAPM TG18 report. *Med Phys*. 2005;32:1205-1225.

19. Digital Imaging and Communications in Medicine. *PS 3.14-2011: Part 14: Grayscale Standard Display Function*. National Electrical Manufacturers Association; 2011.

20. Society of Motion Picture and Television Engineers. *SMPTE RP 133–1991: Specifications for Medical Diagnostic Imaging Test Pattern for Television Monitors and Hard-Copy Recording Cameras (R1999)*. Society of Motion Picture and Television Engineers; 1991.

21. The Joint Commission. Revision to Recently Issued Standards for Organizations Providing Fluoroscopy Services, Issued December 17, 2018 https://www.jointcommission.org/-/media/tjc/documents/standards/prepublications/cah_fluoroscopy_updates_prepub_jan2019_emb.pdf?db=web&hash=DE2AD46A5556A11E2024CC1E002F1E48. Accessed February 2021.

22. Gress DA, Dickinson RL, Erwin WD, et al. AAPM medical physics practice guideline 6.a.: performance characteristics of radiation dose index monitoring systems. *J Appl Clin Med Phys*. 2017;18(4):12-22.

23. Joint commission perspectives, Sentinel event definition and chapter revised, July 2021, Page 18, Volume 41, Number 7.

24. National Council on Radiation Protection and Measurements. Radiation dose management for fluoroscopically-guided interventional medical procedures. NCRP Report No. 168. National Council on Radiation Protection and Measurements, Bethesda, MD.

25. DeLorenzo MC, Goode AR. Evaluation of skin dose calculation factors in interventional fluoroscopy. *J Appl Clin Med Phys*. 2019;20:159-168.

26. International Electrotechnical Commission (IEC2010). Medical Electrical Equipment–Part 2–43: Particular Requirements for the Basic Safety and Essential Performance of X-ray Equipment for Interventional Procedures, IEC 60601-2-43 ed2.0, International Electrotechnical Commission, Geneva, 2010

27. Lin PJ. Preparation for peak skin dose estimation. *J Appl Clin Med Phys*. 2018;19:370-407.

28. American Society for Testing and Materials International. *ASTM F3094-1: Standard Test Method for Determining Protection Provided by X-Ray Shielding Garments Used in Medical X-ray Fluo-*

roscopy from Sources of Scattered X-Rays. American Society for Testing and Materials International; 2014.

29. Seissl J, Eschenbacher H, inventors, Siemens Aktiengesellschaft, assignee. X-ray diagnostic apparatus with a filter device. US patent 5680435A. October 21, 1997.

30. Inaba Y, Chida K, Kobayashi R, Zuguchi M. A cross-sectional study of the radiation dose and image quality of X-ray equipment used in IVR. *J Appl Clin Med Phys*. 2016;17:391-401.

31. International Electrotechnical Commission. *International Standard. IEC 61223-3-1: Evaluation and Routine Testing in Medical Imaging Departments. Part 3-1: Acceptance Tests - Imaging Performance of X-Ray Equipment for Radiographic and Radioscopic Systems*. International Electrotechnical Commission; 1999.

32. Leeds TOR 18FG Fluoroscopy Phantom. Leeds Test Objects website. https://www.leedstestobjects.com. Accessed November 4, 2020.

33. National Electrical Manufacturers Association. *NEMA XR 21–2000: Characteristics of and Test Procedures for a Phantom to Benchmark Cardiac Fluoroscopic and Fluorographic Performance*. National Electrical Manufacturers Association; 2000.

34. Digital Subtraction Angiography (DSA) Phantom Model 76–710. Supertech website. https://www.supertechx-ray.com/QualityControlPhantoms/76-710.php. Accessed November 4, 2020.

35. High M, Cohen G, Lin PJ, et al. *AAPM Report No. 15: Performance Evaluation and Quality Assurance in Digital Subtraction Angiography*. American Association of Physicists in Medicine; 1985.

36. Goode AR, Snyder C, Snyder A, Collins P, DeLorenzo M, Lin PJ. Signal and contrast to noise ratio evaluation of fluoroscopic loops for interventional fluoroscope quality control. *J Appl Clin Med Phys*. 2019;20:172-180.

37. Walz-Flannigan A, Weiser J, Goode AR, et al. *AAPM Report No. 248: Interoperability Assessment for the Commissioning of Medical Imaging Acquisition Systems*. American Association of Physicists in Medicine; 2019.

38. American College of Radiology, American Association of Physicians in Medicine. ACR–AAPM Technical Standard for Diagnostic Medical Physics Performance Monitoring of Fluoroscopic Equipment. Updated 2016. https://www.acr.org/-/media/ACR/Files/Practice-Parameters/RadEquip.pdf. Accessed November 3, 2020.

39. Vano E, Gonzalez L, Beneytez F, Moreno F. Lens injuries induced by occupational exposure in non-optimized interventional radiology laboratories. *Br J Radiol*. 1998;71:728-733.

40. US Food and Drug Administration, Code of Federal Regulations Title 21. *Performance Standards for Ionizing Radiation Emitting Products, Section 1020.32: Fluoroscopy equipment. (g) Source-to-Skin Distance*. US Food and Drug Administration; 2019.

41. Honey I, Rose A, Baker C, et al. IPEM Topical Report: an evidence and risk assessment based analysis of the efficacy of tube and generator quality assurance tests on general x-ray units. *Phys Med Biol*. 2018;63:245011.

42. Worrall M, Shaw D, Baker C, et al. IPEM Topical Report: an evidence and risk assessment based analysis of the efficacy of quality assurance tests on fluoroscopy units – part I; dosimetry and safety. *Phys Med Biol*. 2019;64:195011.

How to cite this article: Lin P-JP, Goode AR, Corwin FD, et al. AAPM Task Group Report 272: Comprehensive acceptance testing and evaluation of fluoroscopy imaging systems. *Med Phys*. 2022;49:e1–e49.

https://doi.org/10.1002/mp.15429

APPENDIX A: SAMPLE ACCEPTANCE TESTING FORM

PAGE: 1 of 8

Fluoroscopy Imaging Equipment Evaluation and Survey Report
Summary

Check if this is for: ☐ **Annual Test**   ☐ **Acceptance Tests**
☐ **Post Repair, Replacement of Component**

Date of Survey:	Contact Person:	☏	(123) 456-7890
Date of Report:	Physicist :	☏	(234) 567-8910

Hospital Unit ID:		**Facility Name:**	
Manufacturer:		Facility Address:	
Model:			
Date of Manufacture:	December 2009	Department ☏	(345) 678-9101
Functional Location Number:		Examination Room ☏	(678) 910-1234
Facility Type:	Hospital	State Facility ID:	
Next Inspection Due (mmm/YYYY):		State Equipment ID:	

	Manufacturer	Model Name/Number	Calibration Due Date	NOTE
Detector Assembly				
Primary Detector				
Detector #1				
Detector Assembly				
Detector #1				

Summary of Physics Tests

	Checklist (Operator Protection, Patient Protection, Equipment, and Area Survey)	Results: Pass, Fail, or N/A
1	Tube Output: Fluoroscopy - Tube Potential Accuracy	Pass
2	Tube Output: Acquisition Mode - Tube Potential Accuracy	Pass
3	Tube Output: Acquisition Mode - HVL	Pass
4	Maximum Patient Entrance Exposure Rate	Pass
5	Patient Entrance Exposure Rates	Pass
6	Image Quality Assessment	Pass
7	Collimation and Radiation Field Congruence with the Displayed Image	Pass
8	DAP Meter Accuracy	Pass
9	Displayed Air Kerma Rate Accuracy	Pass
10	Mechanical Alignment of C-arm with the tabletop/pedestal	Pass
	If mechanical misalignment is found, describe the misalignment in detail for corrective actions.	

	Overall Test Result:	Pass

General Comments and Recommendations

Is each test consistent with State, Federal and manufacturer's specifications?	YES ☒	NO

PAGE: 2 of 8

Equipment Information and Check List

Facility Name:		State Facility ID:
Hospital Unit ID:		State Equipment ID:

Flat Panel Image Receptor: FOV and Matrix Size

Field-of-View (FOV)	48 cm	42 cm	32 cm	22 cm	16 cm	11 cm
Matrix Size	1240X960	960X960	1440X1440	1024X1024	720X720	512X512

EQUIPMENT INFORMATION

Control Console/Generator		X-ray Tube:	
Manufacturer:		Manufacturer:	January 0, 1900
Model:		Model:	SX-21
Serial Number:		Serial Number:	
		Maximum kVp:	
		Maximum mA:	

Basic Geometrical Arrangement and Generator Presets

Test Mode: Under Siemens Service Mode		Focal Spot Selected:	Small	
Maximum SID Available	120 cm	Copper Spectral Filter:	0 mm	
SID set for testing:	105 cm	X-ray Tube Current:	20 mA	
Thickness of Patient Mattress:	3 cm	Examination Tabletop:	OUT	
Examination Mode Selected:	Neuro	Source-to-Isocenter:	75 cm from focal spot.	
Fluoroscopy Pulse:	10 p/s	Source-to-Ref. Point:	60 cm from focal spot.	

	YES	NO	N/A
OPERATOR PROTECTION			
1. Does overtable shielding exist?	X		
2. Does undertable shielding exist?	X		
3. Lead aprons are available?	X		
4. Gloves and aprons in good condition?	X		
PATIENT PROTECTION			
1. Gonadal protection provided?			X
2. Dose charts available?			X
EQUIPMENT			
1. X-ray production can occur only w/ primary barrier in place?			X
2. Switches (Foot Pedal, Hand Switches) require constant pressure?	X		
3. Fluoroscopy X-Ray warning sign on unit?	X		
4. 5-minutes cumulative audible exposure signal?	X		
5. All controls, meters, lights and indicators working?	X		
AREA SURVEY			
1. Approved warning sign on door(s)?	X		
2. Equipment Registration form available?	X		
3. Safety procedures posted?	X		
4. Notice to Employees posted?	X		
5. Operators list available?	X		

PAGE: 3 of 8

Equipment Evaluation Data

Facility Name:		State Facility ID:	
Hospital Unit ID:		State Equipment ID:	

Basic Geometrical Arrangement and Generator Presets

Maximun SID Available:	120	cm	SID Employed for Testing:	105	cm
Source-to-Isocenter:	75	cm	Source-to-Detector Point:	60	cm
Source-to-Reference Point:	60	cm	Patient Table+Mattress Thickness:	8	cm
Examination Mode @ Power Up	Neuro, Smooth		Table Height Indicator Set to:	0	cm
Fluoroscopy Pulse:	10	p/s	Examination Tabletop:	OUT	

Test Mode:

(1) Fluoroscopy Tube Potential Accuracy

Copper Filter	Preset kVp	40	50	60	70	80	90	100	110	120	125	
0 mm	Measured kVp		49.96	60.04	69.85	79.18	88.69	97.42	**106.34**	**115.76**		
? Filter	kVp % Error		-0.1	0.1	-0.2	-1.0	-1.5	-2.6	-3.3	-3.5		
0 mm	HVL (mmAl)		1.85	2.15	2.55	2.99	3.39	3.82	4.26	4.69		
Total Filtration (mmAl)												

kVp Percent Error must be less than +/- 10%	Satisfactory

(2) Acquisition Mode

Data Table for kVp Accuracy, Pulse Width, Radiation Output Linearity and Half Value Layer.

	Small Focal Spot at		4	mAs			Large Focal Spot at		40	mAs	
	Focal Spot		Current	Pulse Width			Focal Spot		Current	Pulse Width	
	Small		40	mA	100	ms	Large		200	mA	200	ms
Set kVp	Measured kVp	kVp Percent Error	Pulse Width (ms)		mGy	HVL (mm Al)	Measured kVp	kVp Percent Error	Pulse Width (ms)		mGy	HVL (mm Al)
		#DIV/0!						#DIV/0!				
50	48.41	-3.18	99.46		0.020	2.61	49.41	-1.18	201.1		0.21	2.60
60	60.21	0.35	99.76		0.035	3.32	60.03	0.05	201.4		0.36	3.22
70	70.15	0.21	100.7		0.054	3.86	69.99	-0.01	200.4		0.53	3.83
80	80.23	0.29	99.54		0.077	4.54	80.37	0.46	200.5		0.76	4.44
90	91.03	1.14	99.65		0.104	5.09	91.55	1.72	200.5		1.03	5.07
100	101.23	1.23	100.2		0.136	5.69	102.54	2.54	199.8		1.35	5.67
110	111.33	1.21	100.24		0.167	6.43	113.79	3.45	199.9		1.67	6.24
120	122.43	2.03	100.23		0.211	6.87	122.03	1.69	200		2.03	6.79
		#DIV/0!						#DIV/0!				
		#DIV/0!						#DIV/0!				

(3) Accuracy of Tube Potential

From Table above:

kVp Percent Error must be less than +/- 10%	Satisfactory

(4) Pulse Width Accuracy

	Pulse Width Accuracy Percent Error must be less than +/- 5%			
	Preset Value	Measured Value	% Error	Result
S	100 ms	99.97 ms	-0.03	Satisfactory
L	200 ms	200.45 ms	0.23	Satisfactory

PAGE: 4 of 8

Facility Name:	State Facility ID:
Hospital Unit ID:	State Equipment ID:

(5) Radiation Output Linearity

Set kVp	Output at 4 mAs (mGy)	Output at 40 mAs (mGy)	Radiation Output Ratio ~	10	YES/NO
50	0.020	0.205	10.250		YES
60	0.035	0.355	10.117		YES
70	0.054	0.533	9.865		YES
80	0.077	0.764	9.917		YES
90	0.104	1.034	9.942		YES
100	0.136	1.353	9.949		YES
110	0.167	1.667	9.982		YES
120	0.211	2.029	9.616		YES
125					

Output Ratio must be between: **9.5** and **10.5**

(6) Half Value Layer Measurements

Preset Tube (kVp)	HVL (mmAl) Small Focal Spot	Large Focal Spot
40		
50	2.61	2.60
60	3.32	3.22
70	3.86	3.83
80	4.54	4.44
90	5.09	5.07
100	5.69	5.67
110	6.43	6.24
120	6.87	6.79
125		

At 80 kVp, HVL must be >= 2.9 mm Al

Satisfactory

(7) Radiation Output Linearity

Set kVP: 70

mAs:	5	10	20	30	50	70	100	
mGy:	0.28	0.54	1.09	1.64	2.74	3.85	5.50	
mGy/mAs:	0.055	0.054	0.055	0.055	0.055	0.055	0.055	Max mGy/mAs difference: 0.90%

The output "mGy/mAs" values must not differ by more than 10% of their sum: **Satisfactory**

(8) Patient Entrance Exposure Rate

Test Mode: Under Clinical Operation Mode.

Measurement Geometry	Source-to-Image Receptor Distance:	105 cm	Raise the SID if necessary.	
	Table Height Indicator set to:	-15 cm	Source-to-Detector (IRP)	60 cm
	The Patient Matrress + Table Thickness:	3 cm	Correction Factor to 30 cm	0.64 cm
	Note: Table height at the isocenter is set to "zero" or manually set to show "zero"			

(8-A) Patient Entrance Exposure Rate for Low Fluoroscopy Mode

Examination Program: Neuro Smooth		Fluoroscopy Output Mode: **Low Fluoro**				Output Displayed on Screen (mGy/min)	Output Corrected for 30 cm from Image Receptor (mGy/min)
Fluoroscopy Pulse Rate:	**10** pulses/sec	**Field-Of-View (FOV)**		**32 cm**			
PMMA Thickness (inches)	Tube Potential (kVp)	Tube Current (mA)	Pulse Width (ms)	Spectral Filter (mmCu)	Measured Output at IRP (mGy/min)		
4							0.00
6							0.00
8							0.00
10							0.00
12							0.00
14							0.00
14+ 2mmCu							0.00
14+4 mmCu							0.00
14+6 mmCu							0.00

In Air Measurement.

PAGE: **5 of 8**

Facility Name:		State Facility ID:
Hospital Unit ID:		State Equipment ID:

(8-B) Patient Entrance Exposure Rate for Normal Fluoroscopy Mode

Examination Program: Neuro Smooth		Fluoroscopy Output Mode: **Normal Fluoro**				Output Displayed on Screen (mGy/min)	Output Corrected for 30 cm from Image Receptor (mGy/min)
Fluoroscopy Pulse Rate: **10** pulses/sec		**Field-Ovf-View (FOV)** **32 cm**					
PMMA Thickness (inches)	Tube Potential (kVp)	Tube Current (mA)	Pulse Width (ms)	Spectral Filter (mmCu)	Measured Output at IRP (mGy/min)		
4	68.4	38.9	5.3	0.3	2.87		1.84
6	68.4	39.4	12.5	0.3	6.58		4.21
8	70.0	63.2	12.7	0.2	17.49		11.19
10	80.0	64.8	12.7	0.2	26.33		16.85
12	91.7	64.8	12.7	0.2	40.45		25.89
14	100.9	65.1	18.3	0.2	74.03		47.38
14+ 2mmCu	125.0	64.9	15.1	0.2	106.50		68.16
14+4 mmCu	125.0	64.7	15.0	0.2	106.60		68.22
14+6 mmCu							0.00

In Air Measurement.

(8-C) Patient Entrance Exposure Rate for High Fluoroscopy Mode

Examination Program: Neuro Smooth		Fluoroscopy Output Mode: **High Fluoro**				Displayed Air Kerma Rate (mGy/min)	Output Corrected for 30 cm from Image Receptor (mGy/min)
Fluoroscopy Pulse Rate: **15** pulses/sec		**Field-Of-View (FOV)** **32 cm**					
PMMA Thickness (inches)	Tube Potential (kVp)	Tube Current (mA)	Pulse Width (ms)	Spectral Filter (mmCu)	Measured Output at IRP (mGy/min)		
4	66.4	39.1	7.9	0.3	5.55		3.55
6	66.4	58.1	12.7	0.3	12.77		8.17
8	70.0	63.3	12.8	0.1	42.40		27.14
10	80.8	64.7	12.7	0.1	63.36		40.55
12	93.5	64.7	12.7	0.1	90.21		57.73
14	103.7	65.1	18.2	0.1	161.70		103.49
14+ 2mmCu	125.0	64.9	15.4	0.1	210.00		134.40
14+4 mmCu	125.0	64.9	15.4	0.2	210.90		134.98
14+6 mmCu							0.00
Warning Yellow Light Activated?		**YES.**		Audible Alert Activated?			**YES.**

In Air Measurement.

NOTES:

For acceptance testing, various Field-of-View (FOV) and Fluoroscopy Operation Modes (FOM) need to be tested.

It is convenient to place the radiation detector at the Interventional Reference Point (IRP) or the Patient Exposure Reference Point (PERP) to compare the "Measured Air Kerma Rate" against the "Displayed Air Kerma Rate" in order to estimate the accuracy of the reported IRP Air Kerma Rate.

One of these tables can be employed to assess the DAP Meter Accuracy in Section (11). Although, TG 190 suggests using the detector under the "integral mode" with 10 cm X 10 cm radiation field to account for the DAP-meter accuracy, we may choose to employ "Rate Mode" testing.

PAGE: **6 of 8**

Facility Name:	State Facility ID:
Hospital Unit ID:	State Equipment ID:

(9) Image Quality Assessment

The center slab of the NEMA XR-21 Phantom is employed and sandwitched in the middle of (a total of) 8" PMMA Phantom.

Source-to-Object Distance, SOD: __70__ cm
Source-to-Image Receptor Distance, SID: __105__ cm

The Main Monitor in the Examination Room is evaluated.

Examination Program: Neuro Smooth — Fluoroscopy Output Mode: **Normal Fluoro**
Fluoroscopy Pulse Rate: **10** pulses/sec — **Field-Of-View (FOV) 32 cm**

Field Of View (cm)	kVp	mA	Pulse width (ms)	Spectral Filter (mmCu)	Sector Number I	II	III	IV	High Contrast Resolution (lp/mm)
48	68.4	38.9	11.4	0.3	8	8	6	2	2.0
42	68.4	39.2	11.8	0.3	8	6	6	0	2.8
32	68.4	56	12.8	0.3	8	8	6	0	3.1
22	70.1	62	12.8	0.2	8	8	6	0	4.0
16	75.9	64	12.9	0.2	8	8	8	0	3.7
11	81.2	64.5	12.7	0.2	8	8	4	0	4.3

Examination Program: Neuro Smooth — Fluoroscopy Output Mode: **High Fluoro**
Fluoroscopy Pulse Rate: **15** pulses/sec — **Field-Of-View (FOV) 32 cm**

Field Of View (cm)	kVp	mA	Pulse width (ms)	Spectral Filter (mmCu)	Sector Number I	II	III	IV	High Contrast Resolution (lp/mm)
48									
42									
32									
22									
16									
11									

Examination Program: Neuro Smooth — Fluoroscopy Output Mode: **Low Fluoro**
Fluoroscopy Pulse Rate: **10** pulses/sec — **Field-Of-View (FOV) 32 cm**

Field Of View (cm)	kVp	mA	Pulse width (ms)	Spectral Filter (mmCu)	Sector Number I	II	III	IV	High Contrast Resolution (lp/mm)
48									
42									
32									
22									
16									
11									

PAGE: 7 of 8

Facility Name:		State Facility ID:
Hospital Unit ID:		State Equipment ID:

(10) Collimation and Radiation Field Congruence with the Image Displayed.

Source to Table Top Distance (cm): **60**	Magnification	2 % of SID
Source to Image Receptor Distance (cm): **105**	Factor: **1.75**	2.1 mm
		4 % of SID
		4.2 mm

		Distance at the edge of fluoresent Screen Placed on Table (mm)	Distance Displayed on Monitor (mm)			Not to Exceed 2% of SID		Not to Exceed 4% of SID	
				Displacement at Image Receptor (mm)					
				Actual	%		%Total Displacement		
48 cm FOV	Head-end	85	84	1.75	0.17%	Satisfactory	Head-Foot Direction		
	Foot-end	87	86	1.75	0.17%	Satisfactory	0.33%	Satisfactory
	Left Side	114	112	3.50	0.33%	Satisfactory	Left-Right Direction	
	Right Side	110	108	3.50	0.33%	Satisfactory	0.67%	Satisfactory
42 cm FOV	Head-end	87	86	1.75	0.17%	Satisfactory	Head-Foot Direction	
	Foot-end	87	89	-3.50	-0.33%	Satisfactory	0.50%	Satisfactory
	Left Side	87	86	1.75	0.17%	Satisfactory	Left-Right Direction	
	Right Side	87	86	1.75	0.17%	Satisfactory	0.33%	Satisfactory
32 cm FOV	Head-end	65	64	1.75	0.17%	Satisfactory	Head-Foot Direction	
	Foot-end	65	63	3.50	0.33%	Satisfactory	0.50%	Satisfactory
	Left Side	65	63	3.50	0.33%	Satisfactory	Left-Right Direction	
	Right Side	65	63	3.50	0.33%	Satisfactory	0.67%	Satisfactory
22 cm FOV	Head-end	45	46	-1.75	-0.17%	Satisfactory	Head-Foot Direction	
	Foot-end	47	46	1.75	0.17%	Satisfactory	0.33%	Satisfactory
	Left Side	47	46	1.75	0.17%	Satisfactory	Left-Right Direction	
	Right Side	47	46	1.75	0.17%	Satisfactory	0.33%	Satisfactory
16 cm FOV	Head-end	30	32	-3.50	-0.33%	Satisfactory	Head-Foot Direction	
	Foot-end	35	32	5.25	0.50%	Satisfactory	0.83%	Satisfactory
	Left Side	35	32	5.25	0.50%	Satisfactory	Left-Right Direction	
	Right Side	30	32	-3.50	-0.33%	Satisfactory	0.83%	Satisfactory
11 cm FOV	Head-end	22	23	-1.75	-0.17%	Satisfactory	Head-Foot Direction	
	Foot-end	24	23	1.75	0.17%	Satisfactory	0.33%	Satisfactory
	Left Side	25	23	3.50	0.33%	Satisfactory	Left-Right Direction	
	Right Side	23	22	1.75	0.17%	Satisfactory	0.50%	Satisfactory

	Collimator Regulatory Questions	YES / NO / NA
1.	Can the x-ray field be collimated to less than 5 cm x 5 cm ?	YES
2.	Minimum source to skin distance ? (cm)	20
		Satisfactory

PAGE: 8 of 8

Facility Name:		State Facility ID:
Hospital Unit ID:		State Equipment ID:

(11) DAP-Meter Accuracy

Measurement Geometry	Source-to-Image Receptor Distance:	105 cm	Raise the SID if necessary.	
	Table Height Indicator set to:	-15 cm	Source-to-Detector (IRP)	60 cm
	The Patient Matrress + Table Thickness:	3 cm	Detector located at IRP.	
	Note: Table height at the isocenter is set to "zero" or manually set to show "zero"			

TG 190, Using Integration of Air Kerma Dose for DAP-Meter Accuracy Evaluation.

Examination Program:	Neuro Smooth	Fluoroscopy Output Mode:	**Normal Fluoro**		**Collimate To:**
Fluoroscopy Pulse Rate:	**10** pulses/sec	**Field-Of-View (FOV)**		**32 cm**	10 cm X 10 cm

Attenuator	Tube Potential	Tube Current	Pulse Width	Pulse Rate	Copper Filter
9.0 mmCu	92.3 kVp	64.8 mA	12.7 ms	10 p/s	0.2 mm

		DAP-Meter Displayed Values		External Calibration Detector Reading				
Initial Value		mGy	μGy-m^2	mGy	mGy-cm^2	TG 190 Correction		
		1647	25455.9			Air Kerma	DAP Reading	
30 second Exposure	#1	1677	25736.5	33.32	3332	1.10	1.16	
		30	280.6					
	#2	1706	26014.4	34.12	3412	1.15	1.19	
		29	277.9					
	#3	1736	26298.5	32.99	3299	1.09	1.14	
		30	284.1					

Alternative to TG 190, Using Dose Rate Mode For DAP-Meter Accuracy Evaluation.

Examination Program:	CardiacCombo	Fluoroscopy Output Mode:	**Normal Fluoro**		
Fluoroscopy Pulse Rate:	**15** pulses/sec	**Field-Of-View (FOV)**		**20 cm**	

	PMMA Thickness (inches)	Tube Potential (kVp)	Tube Current (mA)	Measured Pulse Width (ms)	Spectral Filter (mmCu)	Measured Output at IRP (mGy/min)	Output Displayed on Screen (mGy/min)	TG 190 Correction Factor
In Air Measurement.	4	65	13.0	10.1	0.9	6.56	6.9	1.05
	6	69	14.5	8.0	0.6	11.86	16.5	1.39
	8	77	15.6	8.4	0.3	43.17	58.9	1.36
	10	87	21.0	12.0	0.1	82.95	116.0	1.40
	12	112	21.0	12.0	0.2	116.91	167.0	1.43
	14	120	14.7	9.1	0.1	120.08	169.0	1.41
	16	120	14.7	9.1	0.1	120.13	169.0	1.41
	14+1/8" Pb	125	14.0	9.1	0.1	120.58	169.0	1.40
							Average	1.36

Note 1. Correction factor of >1 means the displayed "air kerma" or "air kerma rate" is lower than measured value.

Note 2. Correction factor of <1 means the displayed "air kerma" or "air kerma rate" is higher than measured value.

Note 3. The average Correction factor is 1.36. TG 190 specifies the tube potential should be ~90 to 100 kVp.

Note 4. Thus, correction factor of either 1.40 or 1.43 should be selected in this case.

APPENDIX B: GENERATOR TEST POINTS

The purpose of this semi-invasive test is to evaluate the waveforms of tube potential and tube current. In so doing, the balance and/or difference between anode and cathode tube potentials can be assessed. In addition, the pulse height of the tube potential and tube current over a prolonged exposure time (up to ~15 s) can be evaluated, and fluctuations in pulse heights in the kV waveform can be observed rather than the radiation exposure train obtained with the radiation detector/probe.

Decades ago, generator-related physical parameters such as the tube potential (kV, kV), tube current (mA), and exposure time (in single exposure or in pulse width [ms]) were measured using an invasive approach, utilizing a high-tension voltage divider and a storage oscilloscope. With the introduction of medium-frequency inverter-type generators, these generator parameters could be more accurately delivered or produced than with the previous generation of generators.

test points varies depending on the specific generator in question. Some systems require entering into service mode and enabling or disabling certain service key switches, whereas other may have no specific precautionary measures.

Once the test points are located, the following generator parameters can be evaluated: tube potentials (kV_{anode}, $kV_{cathode}$, kV_{total}), tube current (mA), and exposure time (ms). The scaling factors for the tube potential (e.g., 1 volt = 10 kV) and tube current (e.g., 1 volt = 10 mA or 1 volt = 100 mA) must also be obtained.

To use this generator test point method, the instrument must have at least a 25- to 50-MHz dual-beam storage oscilloscope and appropriate probes.

APPENDIX C: CONVENIENCE TABLE FOR IN-AIR MEASUREMENTS

To facilitate various measurements and to comply with in-air measurements, a homemade table was fabricated in a machine shop, as shown below:
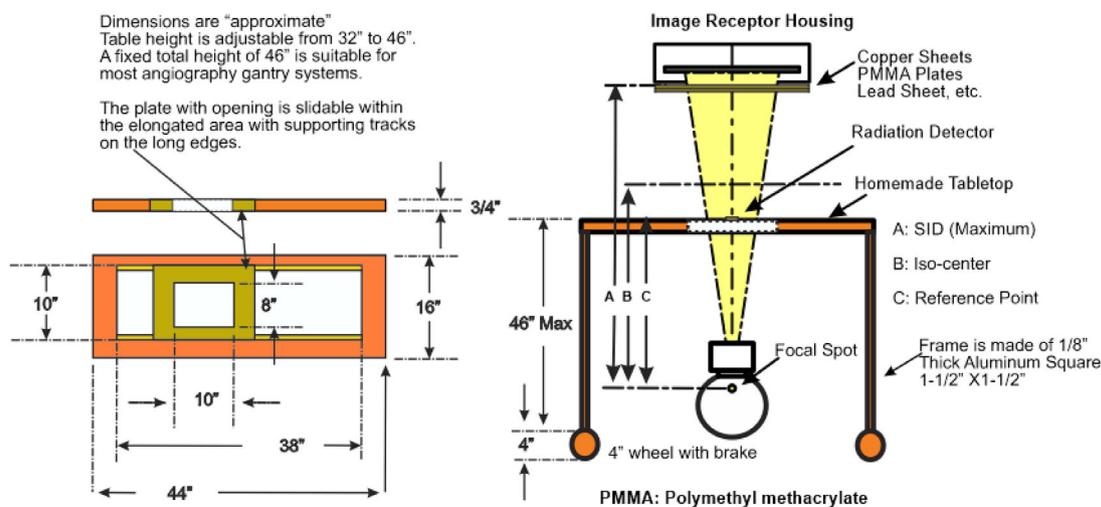
On the other hand, when noninvasive SSDS became available, tube voltage, exposure time, and radiation dose could be measured in one exposure. Although SSDS are convenient, the wave form provided with these systems is not the voltage (or current) waveform. Rather, it is the radiation waveform, which reflects the power loading of the X-ray tube and is influenced by both the tube voltage and current. The exposure time is derived from the radiation waveform, and its accuracy is acceptable when the exposure time is longer than approximately 15–20 ms; for exposure times shorter than 20 ms, and especially for those shorter than 10 ms, the accuracy is not at the desired level of better than ±5% tolerance. For pulse width measurements, most SSDS may not be suitable measurement devices because of the operating frequency of SSDS and the memory available.

For most generators, the test points are in the equipment cabinet and can be accessed with assistance from the service engineers. The process to access these

The table can be designed to have either a fixed or adjustable height (corresponding to the *Y*-axis shown in Figure 1 of the main text). For most interventional X-ray equipment systems, an acceptable total height is a fixed 40 inches. For the table shown above, the maximum total height (including the wheels) is 50 inches, and the height can be adjusted in 1-inch increments. The same table can be used for mobile C-arm equipment testing; the mobile C-arm gantry can be raised to meet the required geometry to perform the measurements described in this report.

The plate with 8-inch × 10-inch opening, shown on the left of the drawing, rides on a track in the tabletop (16 inches × 44 inches) for *X*-axis direction movement. The table as a whole is moved into position in the *Z*-axis. The 8-inch × 10-inch plate is equipped with a transparency film for inkjet printers (e.g., 3M's product number CG3460). The transparency film is employed to hold the SSDS, the radiation probe, or an ionization chamber.

A table width of 44 inches is necessary to accommodate interventional X-ray systems that have the X-ray tube assembly installed on the primary C-arm (the A-plane) such that the cathode–anode direction is perpendicular to the C-arm, in parallel with the *X*-axis.

APPENDIX D: CNR OPTIMIZATION

One of the concepts involved in the logic design of automatic dose rate control (ADRC) fluoroscopy curves is CNR optimization, as described in US Patent 6222907B1.[1] Traditional logic is based on SNR optimization or constant input dose (or dose rate) to the image receptor, and most image quality evaluations and phantoms are based on the SNR optimization concept that the input dose is kept constant by the fluoroscopy ADRC control logic. However, with innovations and technological advancements such as higher X-ray tube heat capacity and more sensitive image receptors, there has been a philosophical shift in fluoroscopy ADRC logic design. Many new cardiovascular (and most fluoroscopy imaging) systems are shifting away from SNR optimization operation logic to CNR optimization, which offers acceptable patient exposure.[2] This shift in ADRC logic design, in turn, may require a change in acceptance testing and phantom design.

The CNR optimization ADRC logic is designed to a predetermined CNR tailored for a specific clinical examination or procedure. When the type of examination or procedure is selected, the ADRC control logic is prepared with certain boundary conditions that attempt to optimize CNR for the selected procedure. Some of these predetermined parameters are as follows:

- the expected motion of the anatomy (e.g., heart walls), to determine the pulse width, fluoroscopy pulse rate, and acquisition frame rate;
- the anatomy itself/the organ(s) to be investigated, including the intrinsic contrast scale of organs versus surrounding anatomy (e.g., the lungs, mediastinum, and spine in chest cavity);
- the contrast agent used in angiography, which may be iodine-based (k-absorption edge of 33.17 keV) or a barium-sulfate compound (k-absorption edge of 37.44 keV); this factor predominantly determines the optimal tube potential that will be used;
- the expected flow rate of circulation of contrast media for programmed stepping imaging (typically, stepping is necessary to follow the imaging areas from the abdomen to the pelvis to the lower extremities in visceral angiographic studies);
- the size and makeup of the guide wire, catheter, and stent. These items, when intended for use in angiography, are composed of medical-grade stainless steel or chromium–cobalt alloys. Iron mixed with carbon to produce steel is the main component of stainless steel, along with elements such as chromium, nickel, molybdenum, silicon, aluminum, and carbon. Manipu-

lation of the tube potential is used to optimize visualization of the guide wire for different materials.

The protocols designed for each specific procedure are created and analyzed based on literally thousands of individual cases. It would be difficult if not impossible to evaluate such comprehensive and complex CNR optimization ADRC logic design. To evaluate the performance of a preprogrammed procedure, an appropriate phantom must therefore be designed and fabricated.

APPENDIX E: POSITIONAL PARAMETER VERIFICATION OF INTERVENTIONAL X-RAY EQUIPMENT

The radiation dose delivered to the skin of the patient during an interventional radiology or cardiac catheterization procedure is directly correlated with the potential for deterministic skin effects. The point at which the X-ray beam enters the patient is therefore of paramount importance for determining the localized peak skin dose. All modern fluoroscopic equipment is capable of monitoring, displaying, and recording the geometrical parameters that define the position of the image receptor during an exposure. Likewise, the equipment will calculate an air kerma value at a manufacturer-defined point in space between the X-ray source and the imaging plane, referred to as the PERP. These parameters are all saved to the RDSR file, which can be viewed on a structured report viewer.

To accurately determine the peak skin dose and the location on the skin of this dose, the precise orientation of the X-ray imaging system must be understood. The parameters involved include:

- the orientation of the patient on the examination table,
- the primary angulation of the X-ray source to the left or right of the patient,
- the secondary angulation of the X-ray source in the cranial or caudal plane of the patient,
- the X-ray source-to-imaging plane distance (SID),
- the X-ray source-to-patient entrance distance (SPD),
- the longitudinal position of the patient (left/right) relative to the X-ray source,
- the lateral position of the patient (head/foot) relative to the X-ray source, and
- the manufacturer-specified PERP location between the source and image receptor

The purpose of this appendix is to outline a methodology to determine the accuracy of the geometrical parameters displayed to the user versus those recorded to the RDSR.

Materials: Tools for determining rotational accuracy:

- plastic framing square (commonly used by carpenters), with BBs attached at the three corners of the triangle,

TABLE E1 Parameters for gantry geometrical evaluation

Positional parameter	Suggested value
RAO/LAO (°)	0
Cranial/caudal (°)	0
If ceiling mounted, rotation around mounting point (°)	0
SID (mm)	Maximum
Table height (mm)	Near isocenter
Table travel left to right (mm)	Near center

RAO, right anterior oblique; LAO, left anterior oblique.

- cross-line laser alignment pointer (commonly used by carpenters); should include a sagittal and coronal beam,
- plastic ruler, and
- 18-inch level.

Method: Assess physical/displayed positional parameters

1. On the acquisition computer, create a new patient exam and use a unique name that can be transferred to and later identified on the in-house PACS or other means for reading the RSDR file. Select a standard digital acquisition program.
2. Position the C-arm in its most basic configuration using the suggested parameters shown in Table E1.

Note that the manner in which these parameters are displayed to users will vary across systems. Users must familiarize themselves with these differences in display.

3. Establish the Center of rotation.
   a. Ensure that the tabletop is level in both the lateral (Z) and longitudinal (X) dimensions.
   b. Define a centerline extending the entire length of the table.
   c. Establish a center-of-rotation axis with an attenuating rod placed in the center of the imaging FOW. Adjust the table height and longitudinal position until the rod stays in the center of the image while the C-arm is rotated around the table.
4. Ensure table motion accuracy.
   Table E2 provides a reference list of the gantry and table positions at which exposures should be made for verification of the geometric parameters. Reference to Table E2 will be made throughout the following text.
   a. Collect and/or save a digital fluoroscopic run at this location (Table E2, line 1).
   b. Position the laser pointer on the table such that the sagittal beam is along the centerline of the table and the coronal beam is at the height of the

center of rotation. (The characteristics and/or size of the laser pointer might place the coronal beam a couple of cm above the center of rotation. Note the difference.)
   c. Tape a ruler horizontally on the C-arm gantry, centered at the cross-point of the laser sagittal and coronal beams.
   d. Move the table +10 cm in the longitudinal direction and verify that this motion is correctly recorded on the in-room display.
   e. Collect and/or save a digital fluoroscopic run at this location (Table E2, line 2).
   f. Repeat step (c), this time moving the table −10 cm in the longitudinal direction.
   g. Collect and/or save a fluoroscopic run at this location (Table E2, line 3).
   h. Return the table to the central position and tape the ruler in the vertical direction on the C-arm gantry.
   i. Raise and lower the table ±10 cm and verify that this motion is correctly recorded on the in-room display.
   j. Collect and/or save a digital fluoroscopic run at each location (Table E2, lines 4–5).
   k. Reposition the laser off of the table so that the sagittal beam will now cross the table in the longitudinal direction near the center of the imaging plane.
   l. Tape the ruler along the axis of the table and centered to the laser beam.
   m. Move the table ±10 cm in the lateral dimension and verify that this motion is correctly recorded on the in-room display.
   n. Collect and/or save a digital fluoroscopic run at each location (Table E2, lines 6–7).
5. Ensure center position accuracy.
   a. Return the gantry setup to the parameters described in Table E1.
   b. Place the framing square on the table so that the BBs on the vertical axis are normal to the imaging plane.
   c. Carefully position the triangle until an image is yielded with the BBs superimposed. Any displacement of the BBs could indicate an inaccuracy in the gantry rotation.
   d. Collect and/or save a digital fluoroscopic run at this location (Table E2, line 8).
6. Ensure RAO/ LAO accuracy.
   a. Rotate the C-arm 45° in the RAO direction.
   b. Place the framing square on the table so that the BBs on the hypotenuse are normal to the imaging plane.
   c. Carefully position the triangle until an image is yielded with the BBs superimposed. Any displacement of the BBs in the Y direction could indicate an inaccuracy in the C-arm rotation.

TABLE E2 List of exposures required for verification of gantry positioning

| Exposure | Physical location of the image receptor relative to the patient | | | Table position | | |
	RAO/LAO	Cranial/caudal	Rotation around mounting point[a]	Longitudinal	Lateral	Vertical
1	0	0	Center	Center	Center	Center
2	0	0	Center	+10 cm	Center	Center
3	0	0	Center	−10 cm	Center	Center
4	0	0	Center	Center	Center	+10 cm
5	0	0	Center	Center	Center	−10 cm
6	0	0	Center	Center	+10 cm	Center
7	0	0	Center	Center	−10 cm	Center
8	0	0	Center	Center	Center	Center
9	45° RAO	0	Center	Center	Center	Center
10	45° LAO	0	Center	Center	Center	Center
11	0	45° cranial	Center	Center	Center	Center
12	0	45° caudal	Center	Center	Center	Center
13	0	0	90° to left	Center	Center	Center
14	45° RAO	0	90° to left	Center	Center	Center
15	45° LAO	0	90° to left	Center	Center	Center
16	0	45° cranial	90° to left	Center	Center	Center
17	0	45° caudal	90° to left	Center	Center	Center
18	0	0	90° to right	Center	Center	Center
19	45° RAO	0	90° to right	Center	Center	Center
20	45° LAO	0	90° to right	Center	Center	Center
21	0	45° cranial	90° to right	Center	Center	Center
22	0	45° caudal	90° to right	Center	Center	Center

RAO, right anterior oblique; LAO, left anterior oblique.

[a]If the unit is so equipped.

d. Collect and/or save a digital fluoroscopic run at this location (Table E2, line 9).
e. Repeat for C-arm positions of 45° LAO.
f. Collect and/or save a digital fluoroscopic run at this location (Table E2, line 10).

7. Ensure cranial/caudal accuracy.
   a. With RAO/LAO reset to 0°, rotate the C-arm 45° in the caudal direction.
   b. Place the framing square on the table so that the BBs on the hypotenuse are normal to the imaging plane.
   c. Carefully position the triangle until an image is yielded with the BBs superimposed. Any displacement of the BBs in the Y direction could indicate an inaccuracy in the C-arm rotation.
   d. Repeat for C-arm positions of 45° cranial.
   e. Collect and/or save a digital fluoroscopic run at each location (Table E2, lines 11–12).

8. Ensure overhead gantry rotation accuracy (for ceiling-mounted systems).
   a. With RAO/LAO and cranial/caudal reset to 0°, rotate the gantry 90° to the left around the mounting point.

b. Collect and/or save a digital fluoroscopic run at this location (Table E2, line 13).
c. Repeat steps 6 and 7 for determining the RAO/LAO and cranial/caudal positioning at this gantry angle (Table E2, lines 14–17).
d. Reset RAO/LAO and cranial/caudal to 0° and rotate the gantry 90° to the right around the mounting point.
e. Collect and/or save a digital fluoroscopic run at this location (Table E2, line 18).
f. Repeat steps 6 and 7 for determining the RAO/LAO and cranial/caudal positioning at this gantry angle (Table E2, lines 19–22).

9. Close out the exam and send the RDSR data to a structured report reader.

10. View the RDSR data file on the structured report reader and compare the recorded geometrical position values with those set at the time of measurement. The DICOM parameter names are listed in Table E3. The values from the RDSR file should substantially match those recorded in the room and those in the exam protocol file. Any discrepancies should be noted and discussed with the system engineer.

TABLE E3 DICOM parameters employed for positioning

Geometrical parameter	DICOM tag	Unit	Values	In DICOM header
Distance source to detector	(0018, 1110)	mm	Absolute	√
Distance source to patient	(0018, 1111)	mm	Absolute	√
Positioner primary angle	(0018, 1510)	°	Movement from RAO to vertical is positive	√
Positioner secondary angle	(0018, 1511)	°	Movement from caudal to vertical is positive	√
Patient position	(0018, 5100)	text	HFS, HFP, FFS, FFP, and so on	√
Distance source to isocenter	(0018, 9402)	mm	Absolute	
Tabletop vertical position	(300A, 0128)	mm	Table motion downward is positive	
Tabletop longitudinal position	(300A, 0129)	mm	Table motion toward LAO is positive	
Tabletop lateral position	(300A, 012A	mm	Table motion toward cranial is positive	

FFP, feet-first-prone; FFS, feet-first-supine; HFP, head-first-prone; HFS, head-first-supine; LAO, left anterior oblique; RAO, right anterior oblique.

REFERENCES FOR APPENDIX D

1. Gordon CL III, Relihan GF, inventors; General Electric Co, assignee. Image quality optimization using an X-ray model based optimization. US patent 6222907 B1. April 24, 2001.

2. Dehairs M, Bosmans H, Marshall NW. Implementation of a spatio-temporal figure of merit for new automatic dose rate control regimes in dynamic x-ray imaging. *Phys Med Biol*. 2019;64:045001.